PhD Thesis

Impact of TASK-1 in human pulmonary artery smooth muscle cells - Modulation of the two-pore domain channel by vasoactive agents

Submitted by

Nagaraj Chandran M.Sc

for the Academic Degree of

Doctor of Philosophy

(Ph.D.)

at the

Medical University of Graz

Department of Anesthesiology and Intensive Care Medicine

Under supervision of

Univ.Prof. Dr. Andrea Olschewski MD

(2012)

Dedicated to my parents

Declaration

I hereby declare that this thesis is my own original work and that I have fully acknowledged by name all of those individuals and organizations that have contributed to the research for this thesis. Due acklowledgement has been made in the text to all other material used. Throughout this thesis and in all related publications I followed the guidelines of ''Good Scientific Practice''.

Graz, [date & signature]

ACKNOWLEDGEMENTS

It is my immense pleasure to express my deep and unrestricted gratitude to my mentor Prof. Andrea Olschewski, who with her vast experience, knowledge and patience has guided me throughout the entire course of my study. I shall be always indebt to her for the constant unrestricted support during troublesome times. I am grateful to her for her time, constant support and encouragements for accomplishment of my work during my studies, which greatly helped me to understand my strength and weakness.

My utmost respects and gratitude to Prof Horst Olschewski, who has been instrumental in providing deeper insights which enabled me to understand challenges in this field. I am grateful to all the members of the Department of Pulmonology for supporting me during my courses of study.

I would like to also take this opportunity to thank Tang Bi, Zoltan Balant ,Grazyna Kwapiszewska Malgorzata Wygrecka and Kenneth Weir for there timely and vital help,with the expreiments which made this study possible.

I also take this opportunity to thank my colleagues and whom are my friends at the end of the day. Tang Bi, Zoltan Balant (and his wonderful family), Yingi Li, Diana Zabini, Bence Nagy, Vasile Foris , Slaven Crnkovic and Valentina Biasin for there kindness and grace towards me, which made my life easy in and out side of the lab.

I extend my special thanks to Elisabeth wirnsperger, Maria Helene Schloffer, Sabine Halsegger, Eva-Maria Schwarzl Anna-Maria Mandl, Gudrun Wakonigg and peter blümel. I cannot forget their kindness, help and efforts for keeping friendly working environment.

I am indebted to the Medical University of Graz, the MolMed PhD Programme for funding this work. I would also like to thank Karin Osibow and Claudia Siener who have helped me with all the formalities required to complete this work.

Finally, I would like to take a chance to express my deepest gratitude to my family members for all unquestionable love, patience and understanding that they gave me during these last years.

TABLE OF CONTENTS

Abbreviation:

TASK-1:	TWIK-related acid-sensitive K^+; TWIK, for tandem P domains in a weak inwardly rectifying K^+
KCa:	calcium-activated potassium channels
K_V:	voltage-dependent potassium channels
SrcTK:	non recptor src tyrosine kinase
I_{KN}:	noninactivating K^+ current
K_{2P}:	two-pore domain potassium (K^+) channels
HPV:	hypoxic pulmonary vasoconstriction
PH:	pulmonary hypertension
PAH:	pulmonary arterial hypertension
PAP:	pulmonary arterial pressure
PASMC:	pulmonary arterial smooth muscle cell
Dasatinib:	Src family tyrosine kinase inhibitor
PP3:	inactive analog of PP2
PP2:	selective inhibitor of Src-family tyrosine kinases
CML:	chronic myelogenous leukemia
EGTA:	ethyleneglycol bis(ß-aminoethyl ether)-*N*,*N*,*N*',*N*'-tetraacetic acid
E_m:	resting membrane potential
ET-1:	endothelin-1
FITC:	fluorescein isothiocyanate-conjugated
HEPES:	4-(2-Hydroxyethyl) piperazine-1-ethanesulfonic acid
PKA:	protein kinase A
PKC:	protein kinase C
PLC:	phospholipase C
siRNA:	small interfering RNA
TEA:	tetraethylammonium

SUMMARY:

The role of potassium (K^+) channels in hypoxic pulmonary vasoconstriction has been intensively studied. There is a great interest among research investigators who work on the pulmonary circulation in defining the mechanisms responsible for hypoxic pulmonary vasoconstriction (HPV). HPV plays a large part in matching ventilation and perfusion in the lung. Oxygen-sensitive K^+ channels are known to be a primary response element. However, the molecular mechanisms behind acute hypoxic inhibition of potassium channels, in particular TASK-1, have been frustratingly difficult to elucidate.

We now provide novel finding that non-receptor Src family tyrosine kinases (SrcTK) are vital for the function of potassium channels and consequently for their contribution to the resting membrane potential of human pulmonary artery smooth muscle cells (hPASMCs) and pulmonary vascular tone. We show that the expression of SrcTK in human lung and in primary human PASMCs, is colocalized with the TASK-1 channels in the plasma membrane. Silencing of SrcTK inhibits the K+ channels, leading to the depolarization of resting membrane potential. Moderate hypoxia inhibits active phospho-SrcTK and reduces the co-localization of the TASK-1 channel and phospho-SrcTK in the cell membrane. The physiological effect of SrcTK inhibition is similar to that of hypoxia, where the TASK-1 current is also inhibited and leads to membrane depolarization.

Given the ability of SrcTK to control the gating of these K^+ channels in response to hypoxia, these kinases appear to be key regulatory molecules involved in the intracellular signalling cascade of HPV and setting the basal pulmonary vascular tone. Moreover, dasatinib, was proposed as a second-line therapy for patients with Chronic myelogenous leukemia (CML). Dasatinib a potent inhibitor of the Src family, has been reported to cause pulmonary arterial hypertension (PAH) in CML patients. This PAH tends to resolve rapidly after discontinuation of the dasatinib suggesting that it may not be primarily due to marked cellular proliferation but to chronic vasoconstriction. One can speculate that dasatinib-initiated pulmonary hypertension may relate to our finding that siRNA against SrcTK reduces K+ current and causes depolarization of hPASMCs and results in increased pulmonary arterial pressure.

This study addresses an important physiological question, the cellular signaling responsible for hypoxic inhibition of K+ channels in human pulmonary artery smooth muscle cells and, by extrapolation, for part of the mechanism of hypoxic pulmonary vasoconstriction.

The wider relevance of this work is shown by a recent report that a Src tyrosine kinase inhibitor, dasatinib, can cause reversible clinical pulmonary hypertension.

ZUSAMMENFASSUNG:

Die Rolle von Kalium Kanaele in hypoxishe pulmonale Hypertonie ist sehr intensiv studiert worden. Es gibt eine besondere Interesse in Lungengefaessforschung um die Mechanismen die fuer die hypoxische Vasokonstriktion verantwortlich sind definieren zu koennen. Hypoxische Vasokonstriktion spielt eine grosse Rolle in der Matching fuer Ventillation und Perfusion. Sauerstoff -Sensibel Kalium Kanaele sind in Erste Linie die dafuer Verantwortlich sind. Trotzdem, die molekulare Mechanismen die die akute hypoxische Inhibition der Kalium Kanaele verursaschen waren wahnsinnig Shwierig zu etablieren.

Wir zeigen erstmal dass die Familie nicht-Rezeptoren Src tyrosine Kinase (SrcTK) fuer die Funktion der Kalium Kanaele und zusaetzlich fuer die Membran Potenziell in Ruhe der pulmonal arterieller Glattenmuskelzellen sowie fuer die Pulmonalgefaesstone vital sind. Wir zeigen experimentell dass SrcTK in humane Lunge und in pulmonal arterieller Glattenmuskelzellen kolokaliziert mit TASK-1 in der Plasma Mebrane sind. Silencing der SrcTK hemmert die Kalium Kanaele und verursacht Depolarization der Ruhe Membran Potenziell. Hypoxie hemmert aktive phospho-SrcTK und vermindert die Kolokalizierung der TASK-1 und phospho-SrcTK in die Zellulaer Membrane, Der physiologische Effekt der SrcTK Hemmerung ist aenlich wie beim Hypoxie wo TASK-1 Strom ist auch hemmert und verursacht depolarisierung der Mebrane.

Die SrcTK sind Schluss Molekulen fuer die intrazellulaere Sygnal Kaskaden fuer Hypoxische Vasokonstriktion und basal vaskulaer Tonus in Ruhe, weil die die Kalium Kanaelen kontrollen. Dasatinib, Hemmer der Src Familie ist eine Therapiemoeglichkeit in Zweite Linie fuer chronische Mieloid Leukemie und kann zu pulmonal arterieller Hypertonie (PAH) fuehren. Eine reversibilitaet ist zu beobachten nach diskontinuierung der Therapie, bedeutend dass diese Effekte sind nicht weil die zellulaere Proliferation sondern weil Vasokonstriktion. Spekulierend kann man sagen dass Dasatinib induzierte Lungenhochdruck kann mit unsere Ergebnisse zuhammenhaengen und zwar siRNA gegen SrcTK vermindert Kalium Kanaeler Strom und verursacht deploarizierung der humane pulmonal arterieller Glattenmuskelzellen fuehrend zu erhoehten pulmonar arterieller Druck.

Diese Studie antwortete eine wichtige phisiologische Frage, naemlich wie die zellulaere Sygnalen verantwortlich fuer die hypoxische Hemmerung der Kalium Kanaele in humane pulmonal arterielle Glattenmuskelzellen und teilerweise hypoxische pulmonale Gefaesskonstriktion verantwortlich sind. Der Relevanz dieser Arbeit ist in eine klinische Studie gezeigt worden wo dasatinib, SrcTK Hemmer

Introduction

Introduction

The pulmonary vascular bed is unique compared with most studied systemic vascular beds. During normoxic conditions, the pulmonary circulation is at low pressure – that is, vasodilated – compared with the high-pressure systemic circulation. In the systemic circulation, hypoxemia elicits vasodilatation that increases O_2 delivery to the tissues. In contrast, small resistance arteries in the pulmonary circulation constrict in response to hypoxia This phenomenon is called as hypoxic pulmonary vasoconstriction.

Hypoxic pulmonary vasoconstriction (HPV)

Hypoxic pulmonary vasoconstriction is a physiological response of the small pulmonary arteries that diverts mixed venous blood away from hypoxic alveoli, thus optimizing the matching of perfusion and ventilation and thus preventing arterial hypoxemia. Hypoxic pulmonary vasoconstriction can be defined as the rapid, reversible increase in pulmonary vascular resistance, caused by the contraction of the small muscular pulmonary arteries with an internal diameter of approximately 200 to 600 μm, in response to physiologic levels of hypoxia(Shirai *et al.*, 1986) . Hypoxic vasoconstriction depends starts within seconds of the onset of airway hypoxia by a decrease in alveolar O_2 tension below a threshold fractional inspired O_2 concentration of ~ 10%(Jensen *et al.*, 1992). If only a small region of the lung is hypoxic, HPV can occur without significant effect on pulmonary arterial pressure(Nakanishi *et al.*, 1996) . However, when hypoxia is generalized, as seen with many lung diseases and in high-altitude exposure, the subsequent pulmonary vasoconstriction contributes to pulmonary hypertension, heart failure and death.

Hypoxia appears to activate mechanisms intrinsic to the pulmonary vasculature, which are independent of blood-born factors or influences requiring the central nervous system, as HPV can be demonstrated in isolated perfused lungs and isolated pulmonary arteries(Weissmann *et al.*, 1995, Weir and Archer, 1995). Acute exposure to hypoxia increases the pulmonary arterial pressure in whole animals and in isolated lungs . Hypoxia also causes contraction in isolated pulmonary arteries(Kato and Staub, 1966), as well as in pulmonary artery rings denuded of endothelium(Yuan *et al.*, 1993) and in single isolated smooth muscle cells from resistance pulmonary arteries(Madden *et al.*, 1985, Olschewski *et*

al., 2002), indicating that the basic mechanism of HPV is intrinsic to the vascular wall of pulmonary arteries. An increase of the cytosolic Ca^{2+} concentration ($[Ca^{2+}]_i$) is necessary to elicit constriction of the vessels. In excitable cells, $[Ca^{2+}]_i$ is increased by Ca^{2+} influx through Ca^{2+}-permeable channels and/or by Ca^{2+} mobilization from intracellular Ca^{2+} stores (e.g., endoplasmic/sarcoplasmic reticulum). Observations from the last three decades suggest that sensing and responding acutely to hypoxia are intrinsic to pulmonary artery smooth muscle (PASMCs) and that both intracellular and extracellular Ca^{2+} are important(Robertson *et al.*, 2000, Tolins *et al.*, 1986) .Calcium influx via voltage-dependent Ca^{2+} channels in vascular smooth muscle cells is controlled by the resting membrane potential (E_m) of these cells. E_m is controlled by the potassium permeability, which is determined by the sarcolemmal potassium (K^+) channel conductance. Hypoxia causes both an inhibition of whole cell K^+ current and membrane depolarization in isolated PASMCs(Post *et al.*, 1992, Yuan *et al.*, 1995), leading to opening of voltage-gated calcium-channels and entry of calcium into the cells.

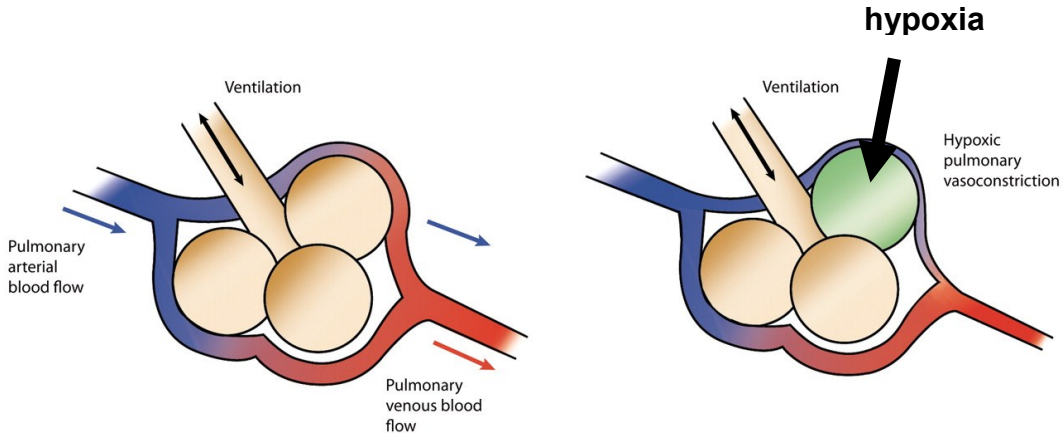

Figure 1.1 Schematic illustration of regional hypoxic pulmonary vasoconstriction (HPV). HPV in the hypoxic atelectatic lung (indicated by the black arrow) causes a redistribution of blood flow away from the hypoxic lung to the normoxic lung, thereby diminishing the amount of shunt flow that can occur through the hypoxic lung. From (Dhillon, 2012).

Potassium (K^+) channels in pulmonary artery smooth muscle cells

The arterial tone is mainly regulated by the membrane potential of pulmonary artery smooth muscle cells. These cells have a resting membrane potential of approximately −65 to −50 mV in vitro, close to the predicted equilibrium potential for potassium (K^+) ions. This means that K^+ channels determine the membrane potential of PASMCs. The opening of K^+ channels in the PASMC membrane increases K^+ efflux, which causes membrane hyperpolarization. This closes voltage-dependent Ca^{2+} channels(VGCC),which in turn decreases Ca^{2+} entry and leading to vasodilatation (Figure 1.2). Conversely, inhibition of K^+ channels causes membrane depolarization, Ca^{2+} entry, cell contraction, and vasoconstriction(Olschewski, 2010)(Olschewski *et al.*, 2006) .

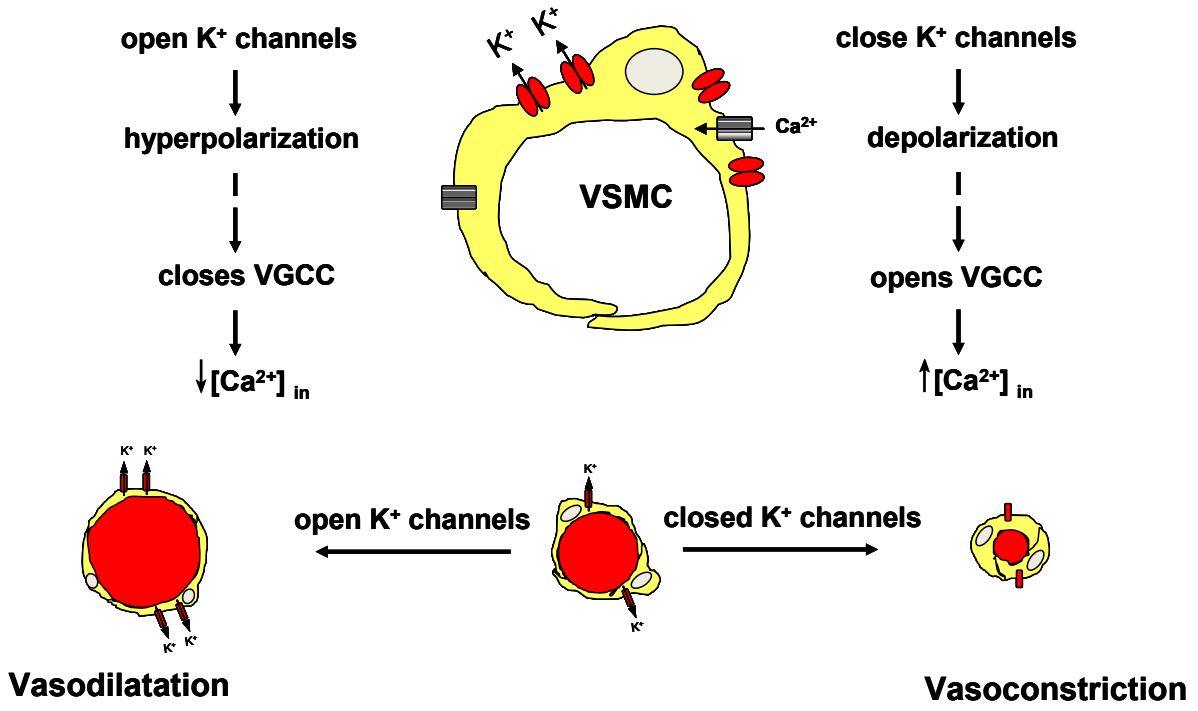

Figure 1.2 Schema of the role of potassium channels for the pulmonary vascular tone. The potassium current in PASMCs reflects activity of many different channels.

At least four classes of potassium channels have been identified in PASMCs: voltage-dependent potassium channels (Kv)(Post *et al.*, 1992, Evans *et al.*, 1996), calcium-activated potassium channels (K_{Ca})(Peng *et al.*, 1999) ATP-sensitive potassium channels (K_{ATP})(Kleppisch and Nelson, 1995)(Weir *et al.*, 2010, Weir and Olschewski, 2006) and the recently discovered group of two-pore domain potassium channels(Weir *et al.*, 2010, Weir and Olschewski, 2006) (Figure 1.3).

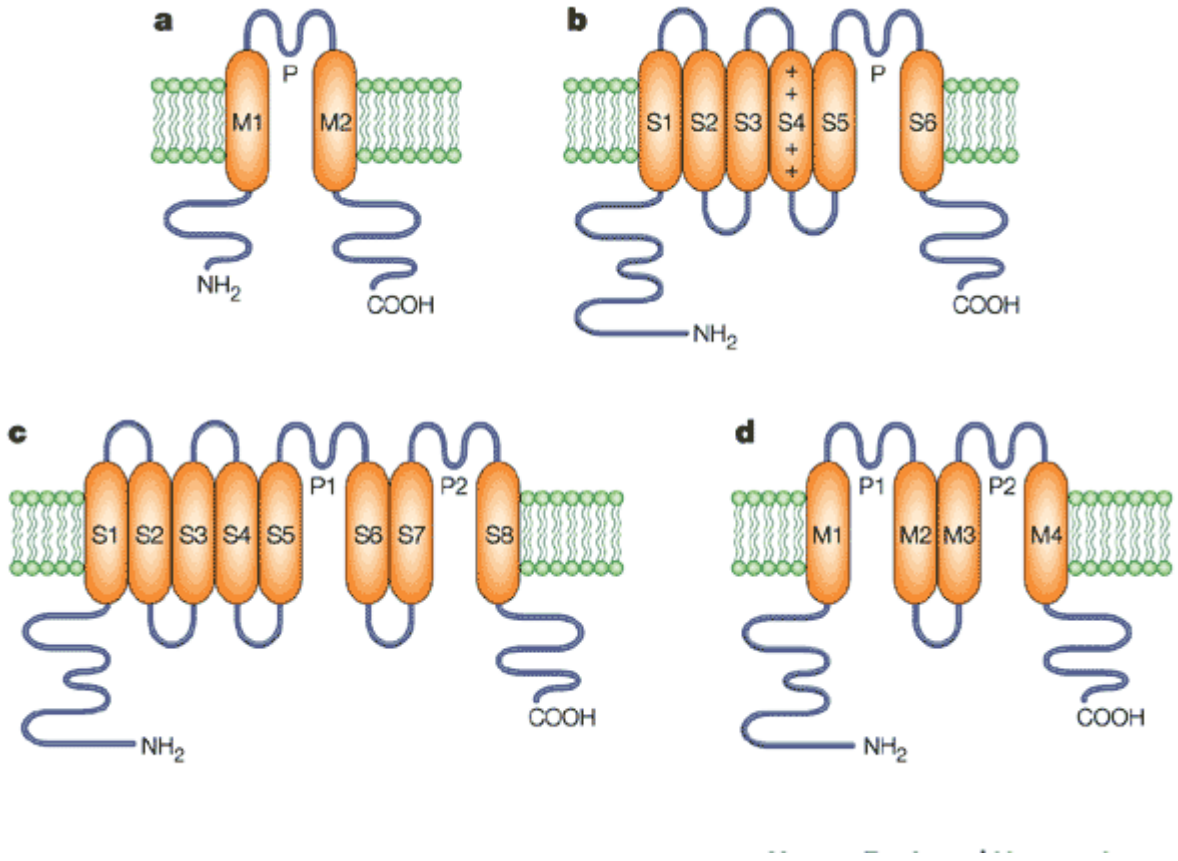

Figure 1.3 The four main classes of potassium channels. **a** Inwardly rectifying K^+ channels (2TM/P channels), which consist of two transmembrane (TM) helices with a P loop between them building the pore. **b** Voltage–gated K^+ channels (6TM/P) **c** 8TM/2P channels, which are hybrids of 6TM/P and 2TM/P, and were first found in yeast. **d** Two-pore domain K+ channels (4TM/2P), which consist of two repeats of 2TM/P channels. 8TM/2P and 4TM/2P probably assemble as dimers to form a channel. 4TM/2P channels are far more common than was originally thought. These so-called 'leakage' channels are also targets of numerous anaesthetics. S4 is marked with plus signs to indicate its role in voltage sensing in the voltage-gated K+ channels. from (Choe, 2002)

The role of potassium (K+) channels in the hypoxic signalling

The most widely distributed structures mediating the effect of changes in oxygen partial pressure (pO_2) are ion channels. Several studies have provided direct evidence that hypoxic vasoconstriction of PASMCs is mediated, at least in part, by the inhibition of one or several K^+ channels leading to cell depolarization, opening of voltage-gated Ca^{2+} channels, and myocyte contraction(Weir and Archer, 1995, Post *et al.*, 1992, Archer *et al.*, 1998, Yuan, 1995).

The potential candidate Kv channel α-subunits that could form O_2-sensitive channels in PASMCs are Kv1.2(Wang *et al.*, 1997), Kv2.1(Hulme *et al.*, 1999)and Kv9.3(Platoshyn *et al.*, 2001).The molecular identification of the specific Kv channels that control E_m is difficult, even with advanced electrophysiological techniques, mainly because of the lack of specific blockers.

The β-subunit could also confer O_2-sensitivity on a K^+ channel. It has been reported that expression of Kv4.2 channels plus Kvβ1.2 subunit in HEK293 cells conferred sensitivity to redox modulation and O_2-sensitivity(Perez-Garcia *et al.*, 1999).

The TASK-1 background potassium (K^+) channel

Background or leak K^+-selective channels, as defined by a lack of time and voltage dependency, play an essential role in setting the resting membrane potential and input resistance in excitable cells. Alteration of K^+ conductance in these cells influences cellular activity via membrane potential changes. Two-pore-domain potassium (K2P) channels have been shown to conduct several leak K^+ currents. This new gene family of K^+ channels has been progressively identified over the last few years(Olschewski, 2010, Weir and Olschewski, 2006) .

Gurney and colleagues showed the TASK-1 expression in smooth muscle cells of the pulmonary artery in a rabbit (Gurney *et al.*, 2003)(Gurney *et al.*, 2002). The authors also demonstrated functional expression of a conductance in these cells that is inhibited by extracellular pH and Zn^{2+} and by the endocannabinoid anandamide, but the conductance was insensitive to intracellular Ca^{2+}, 4-aminopyridine, and quinine. In addition, the noninactivating K^+ current was facilitated by halothane, causing hyperpolarization of pulmonary artery smooth muscle cells. These are properties that closely mimic the

pharmacology of heterologously expressed TASK-1 channels. Our group described for the first time the TASK-1 K^+ background channel in freshly isolated and short term cultured human pulmonary artery smooth muscle cells(Olschewski *et al.*, 2006)

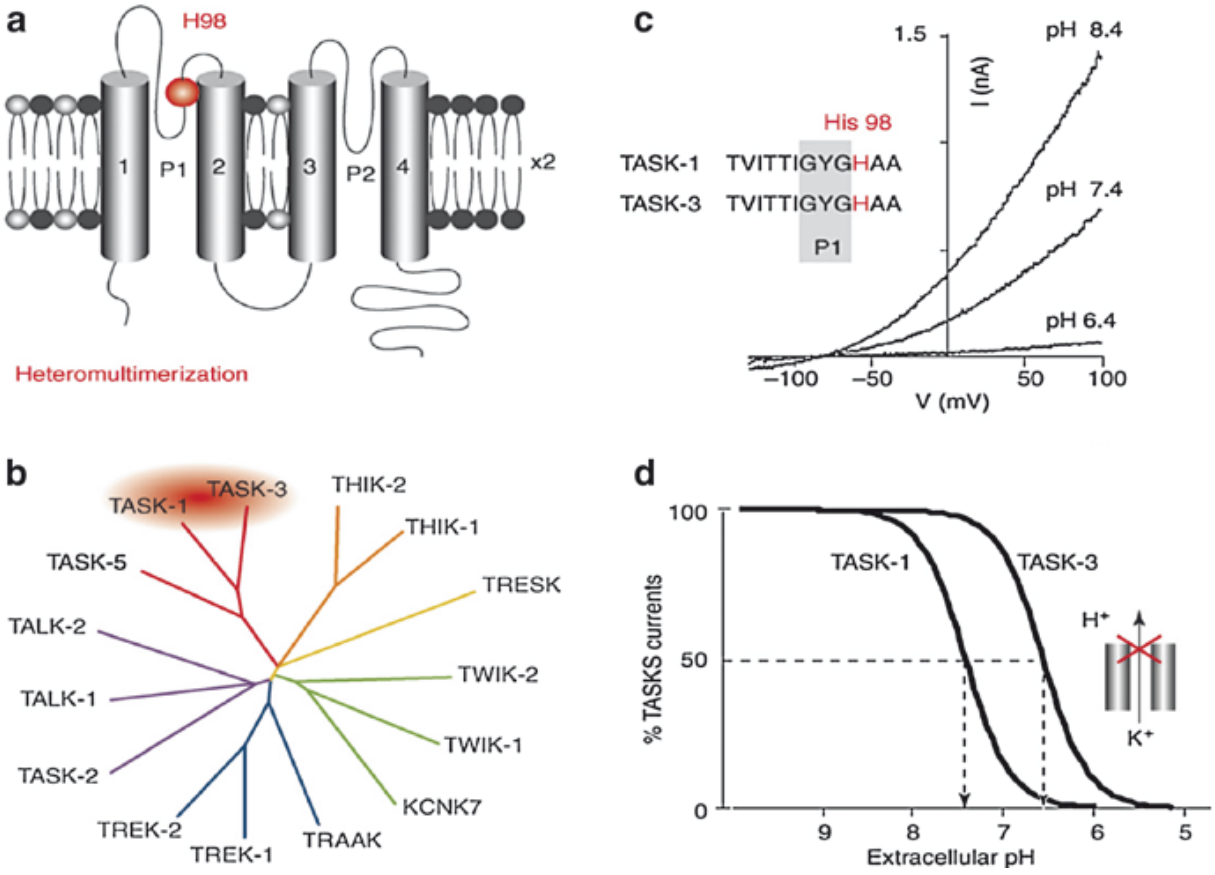

Figure 1.4 The TASK K2P channels. (**a**) The subunits of dimeric K^+ channels each contain four transmembrane segments (4-TMs) and two conserved motifs called the P (pore-forming) domain that forms part of the wall of the channel through which K^+ ions are conducted; these are known as K2P channels. His98 in the P1 domain is involved in sensing pH. (**b**) Fifteen human K2P channel subunits have been identified and are classified into six different structural and functional subgroups. The TASK-1 and TASK-3 subunits share a background K^+ channel activity that is inhibited at extracellular acidic pH. (**c**) Effect of extracellular pH on TASK-1 recorded in a transfected COS cell. TASK channel activity monitored between -120 and 100 mV using a voltage ramp is increased by alkaline extracellular pH (pH 8.4) but inhibited by extracellular acidosis (pH 6.4). This *curve* represents the whole-cell current amplitude (in nA) as a function of the membrane voltage (in mV). The pH sensitivity of the

TASK-1 and TASK-3 channels is dependent on the protonation of His98 in the first pore domain (P1) as shown in (**a**). (**d**) TASK-1 and TASK-3 show different pH sensitivities with a pK of about 7.3 and 6.7 for TASK-1 and TASK-3, respectively. from (Duprat *et al.*, 2007)

Modulation of ion channels

Multiple pathways may exist for hypoxia-induced K channel inhibition. Hypoxic signalling may be related to a) a conformational change of the channel b) a change in cellular (sarcoplasmic or cytoplasmic) redox status, secondary to altered NAD(P)H oxidase- and/or mitochondrial-dependent oxygen radical formation; or c) a decrease in the ratios of the cytosolic redox couples (NAD/NADH; NADP/NADPH; GSH/GSSG), secondary to slowing of mitochondrial electron transfer.

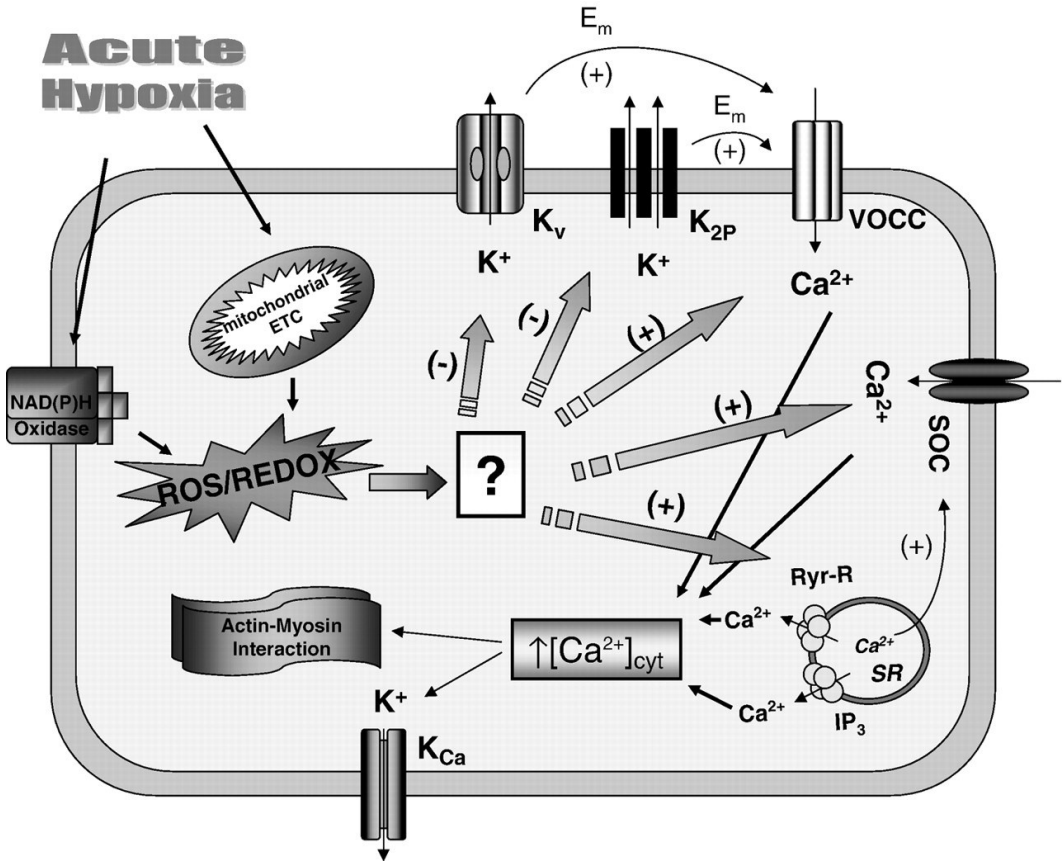

Figure 1.5 Proposed schematic presentation of ion channels involved in acute HPV in pulmonary artery smooth muscle cells (PASMC). In PASMC hypoxia, in part due to altered release of reactive oxygen species (ROS) and/or changes in redox status inhibits voltage-gated K^+ channels (Kv) and two-pore domain K^+ channels (K2P), leading to the depolarization of the membrane (Em) and activation of voltage-operated L-type Ca^{2+} channels (VOCC). Depletion of Ca^{2+} from the sarcoplasmic reticulum opening of store operated channels (SOC) allows for Ca^{2+} influx, termed capacitative calcium entry. Intracellular [Ca^{2+}] is also increased by hypoxia through the activation of SOC or receptor-operated (ROC) Ca^{2+} channels. The hypoxia-induced rise in [Ca2+] then triggers the PASMC contraction. ETC electron transport chain, NAD(P)H oxidase; SR sarcoplasmic reticulum; Ryr-R ryanodine receptors, IP3 inositol-1,4,5-triphosphate receptor; KCa Ca^{2+}-sensitive K^+ channels.from(Weir and Olschewski, 2006).

Modulation of TASK-1

The two-pore domain channel TASK-1 with its biophysical profile of a background K^+ channel could be the perfect candidate for the initiation of hypoxia-induced depolarization in pulmonary artery smooth muscle cells. Our group were able to show the hypoxia sensitivity of the TASK-1 current in primary hPASMCs. Although the mechanisms involved in the hypoxia-induced inhibition of TASK-1 are still not clearly understood, TASK-1 channels may play an important role in the regulation of the resting membrane potential in human pulmonary arteries and eliciting vasoconstriction responses during hypoxia(Olschewski *et al.*, 2006).

In addition, a number of G protein-coupled pathways have been shown to regulate the activity of K2P channels including TASK channels. The most commonly occurring regulation seems to be Gαqmediated inhibition, which is seen for both, TASK and TREK channels (Chen *et al.*, 2006)

.

Src family Tyrosine Kinase (SrcTK) in pulmonary hypertension

Src tyrosine kinase belongs to the non receptor tyrosine kinase family. These enzymes transfer a phosphate group from ATP to the tyrosine residue in a targeted protein. Src tyrosine kinase has nine members: Src, Yes, Fyn, Fgr, Lck, Hck, Blk, Lyn and Frk. They are ubiquitously expressed in many tissues with varying levels. There is a high similarity of aminoacid sequence in between the family members. All SrcTK are structually conserved containing three SH domains (SH2-4), the protein–tyrosine kinase domain (the SH1 domain), and a C-terminal regulatory segment (Figure 1,6). At the N- terminus, Src contains a 14-carbon myristoyl group attached to an SH4 domain, which is a unique domain. Myristoylation facilitates the attachment of Src to membranes,is required for its operation in cells. The SH2 and SH3 domains have three important functions: i) they constrain the activity of the enzyme, ii) they attract proteins that contain SH2 or SH3 ligands and they can bind them to specific cellular locations and finally iii) via these domains other proteins containing SH2 or SH3 ligands can function as substrates for the Src protein–tyrosine kinase. The C-terminal is the regulatory tail. Src activation is dependent on the interaction of different SH domains with each other and a carboxyterminal (C-terminal) domain. Functionally, SrcTK can promote

mitogenic signaling for DNA synthesis, control of receptor turnover, differentiation, actin cytoskeleton rearrangements, motility, and survival.

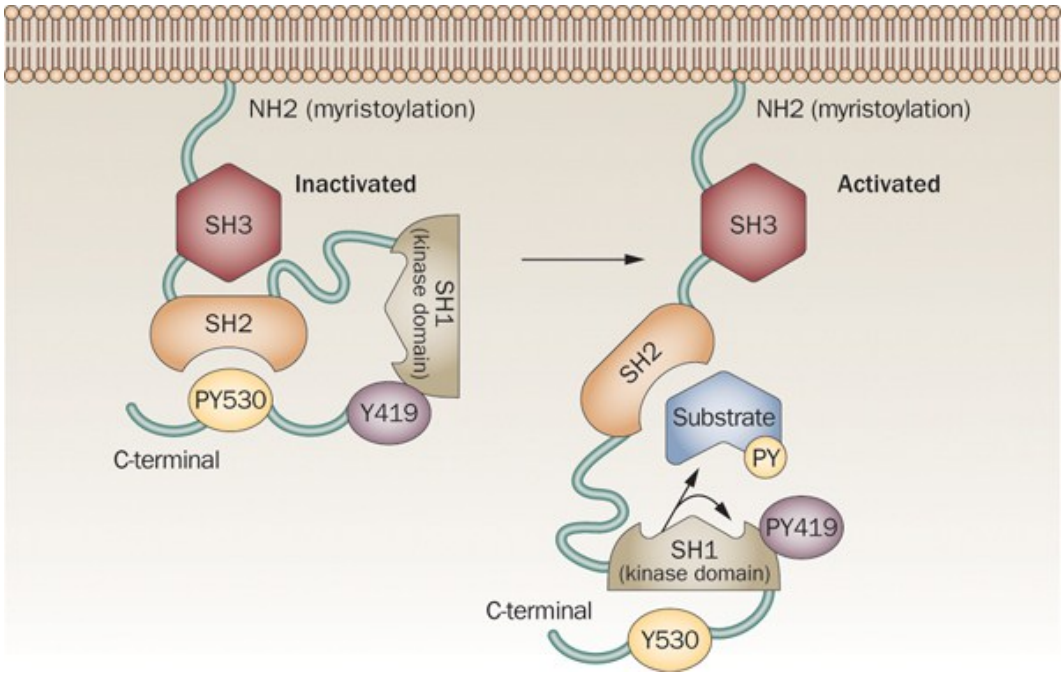

Figure 1.6 The SH4 domin of C-Src is located on the N-terminal region and contains a myristoylation sequence important for its membrane attachment. The SH3 domain is a proline-rich target domain that binds and interacts with other proteins or with c-Src itself. The SH2 domain can recognize phosphorylated tyrosine-containing residues, critical for regulation of Src activity or binding to other tyrosine proteins. The SH1 domain contains the kinase domain as well as tyrosine residue Y419, which is phosphorylated by the kinase domain. Src activity is regulated by the C-terminal tyrosine site Y530 interacting with the SH2 domain. When Y530 is phosphorylated by C-terminal Src kinase, the C-terminus binds to the SH2 domain and inhibits Src activation via changing the configuration of SH2, SH3, and SH2-linker sites; the entire configuration becomes locked and inactive. Dephosphorylation of Y530 by protein tyrosine phosphatases allows the Src SH1, SH2 and SH3 domains to become open and therefore fully activated. from (Kim *et al.*, 2009)

In respect to hypoxic vasoconstriction and vascular remodelling of the pulmonary artery the role of SrcTK is not fully understood. Knock et al showed the activation of major SrcTKs under hypoxia in rat PASMC(Knock *et al.*, 2008b). Moreover, when the pulmonary arteries were preconstricted with prostaglandin F2, the response of hypoxic vasoconstriction was completely inhibited under preincubation with the SrcTK blocker PP2. The study also address the hypoxia induced calcium response and the Rho kinase translocation. Both were completely inhibited after silencing of the major SrcTK family. In addition, they also addressed the down stream signalling, such as hypoxia-mediated actin cytoskeleton rearrangements by phosphorylation of the myosin-binding subunit (myosin phosphatise (MYPT-1)) and myosin regulatory light chain (MLC20) furthermore, the study offers further insights into the role of SrcTK in acute hypoxic changes in rat pulmonary arteries.

Role of SrcTK in pulmonary vascular remodelling is the main topic of current debates. R. M. Tuder et al showed that in lungs of (16)sixteen patients suffering from primary pulmonary hypertension (PPH) the protein expression of C-Src (a member of SrcTK) is significantly down regulated compared to healthy tissue (Tuder *et al.*, 2001). On the other hand, a recent study by Courboulin et al. reports increased levels of phosphor-Src and total Src in lung samples from three PAH patients(Courboulin *et al.*, 2011) . Unfortunately, no further information is given about the etiology of PAH and the concomitant diseases in this particular study. Apart from this result, the study also addressed the downstream signalling of SrcTK, namely the signal transducer activator of transcription 3 (STAT3) proving the role of SrcTK in apoptosis resistance and proliferation of pulmonary artery smooth muscle cells. This effect has been inhibited by treatment of dehydroepiandrosterone (DHEA) which also inversely reverses the regulation of SrcTK and reversed the STAT3 translocation and finally DHEA improves experimental model pulmonary hypertension in mice. Based on the limited number of studies about the role of SrcTK in pulmonary arteries and in pulmonary hypertension further conclusions cannot be drawn from these observations.

The most important finding about the role of SrcTK in human pulmonary arteries comes from recent case reports and clinical studies about cancer patients suffering from chronic myelogenous leukemia (CML)(Dumitrescu *et al.*, 2011, Kantarjian *et al.*, 2010, Kantarjian *et al.*, 2010).Chronic myelogenous leukemia is a chronic disease in which the bone marrow produces too many white blood cells. This chronic myeloproliferative disorder is characterized by a translocation between chromosome 9 and 22: this results in constitutively active BCR-ABL tyrosine kinase. Tyrosine kinase inhibitors (TKI) represent the current treatment of CML. The first–line therapy is Imatinib. However, 20% of patients treated with

Imatinib do not achieve complete cytogenetic levels. The novel tyrosine kinase inhibitor Dasatinib has been found to be associated with higher rates of complete cytogenetic response in Imatinib-resistant chronic-phase CML. Dasatinib is 325 times as potent as imatinib in the inhibition of BCR-ABL kinase in vitro and induces higher and faster rates of cytogenic response in CML. Dasatinib and Imatinib have a different profile of kinase inhibition (Table 1). Apart from the inhibition of the BCR-ABL, Dasatinib also potently inhibits the entire family of SrcTK. Currently, Dasatinib represent the second-line therapy for patients with CML.

Table 1

Imatinib	**Dasatinib**		
ABL	ABL	DDR1	MYT1
ARG	ARG	DDR2	NLK
BCR-ABL	BCR-ABL	ACK	PTK6/Brk
KIT	KIT	ACTR2B	QIK
PDGFR	PDGFR	ACVR2	QSK
DDR1	SRC	BRAF	RAF1
NQO2	YES	EGFR/ERBB1	RET
	FYN	EPHA2	RIPK2
	LYN	EPHA3	SLK
	HCK	EPHA4	STK36/ULK
	LCK	EPHA5	SYK
	FGR	FAK	TA03
	BLK	GAK	TESK2
	FRK	GCK	TYK2
	CSK	HH498/TNNI3K	ZAK
	BTK	ILK	
	TEC	LIMK1	
	BMX	LIMK2	

There is emerging evidence that chronic treatment with Dasatinib may results in increased pulmonary arterial hypertension (PAH) and edema. Unfortunately, the increased pulmonary pressure is not fully reversible after termination of the Dasatinib treatment. This serious side-effect has been described recently as a novel drug-induced PAH. However, the pathomechanism by which Dasatininb or SrcTK inhibition to cause increase in PAP or inhibition of K^+ channels is not clear.

Aims of PhD thesis

1) To elucidate the role of the G protein-coupled pathways for the regulation of the activity of TASK-1 channels

2) To investigate the regulatory mechanisms of TASK-1 channel function in human pulmonary artery smooth muscle cells under hypoxia

3) To characterize if the TASK-1 - hypoxic responsive element is also responsible for the regulation of other oxygen-sensitive potassium channels like Kv or Kca channels in human pulmonary artery smooth muscle cells

4) To study the role of the inhibition of the hypoxic responsive element for maintaining of the resting membrane potential of human pulmonary artery smooth muscle cells

5) To investigate the role of the hypoxic responsive element for the hypoxic induced calcium response in human pulmonary artery smooth muscle cells

6) and finally, to study the relevance of this factor for the pulmonary vascular tone or/and the pulmonary arterial pressure

Methods

Methods

Preparation of human primary pulmonary artery smooth muscle cells (hPASMC) and cell culture

The study protocol for tissue donation was approved by the "Institutional Review Board" of the Medical University of Graz in accordance with the national law and the guidelines on Good Clinical Practice/International Conference on Harmonization. Written informed consent was obtained from each individual patient if appropriate.

Primary SMCs were isolated from human resistance pulmonary arteries of patients (n = 30) undergoing lung surgery for lung cancer without a history of pulmonary vascular disease or arterial hypoxemia or unused donor lungs harvested for lung transplantation. the pulmonary arteries obtained from patients with lung cancer, only those arteries were used which had a distance of at least 5 cm from the cancer tissue. The adventitia of small arteries with diameters of <1mm was carefully removed under a dissection microscopic (Leica, Germany) and media pieces (<1mm^3) were placed onto 75mm flask. The pieces were covered by a drop of culture medium (Lonza SMC Medium; Lonza Group Ltd, Switzerland) for first 24 hours and later filled with culture medium. Cells were maintained at 37°C, medium was initially changed after 24h, and then every 48h thereafter. PASMCs grown on coverslips were used for patch-clamp recordings, intracellular calcium measurements and siRNA transfection. SMC identity was verified by their characteristic appearance in phase-contrast microscopy. The purity of PASMC cultures was confirmed using indirect immunofluorescent antibody staining for smooth muscle-specific isoforms of alpha- smooth muscle actin as shown in figure 2.1 (at least 95% of cells stained positive) and lack of staining for von Willebrand factor.

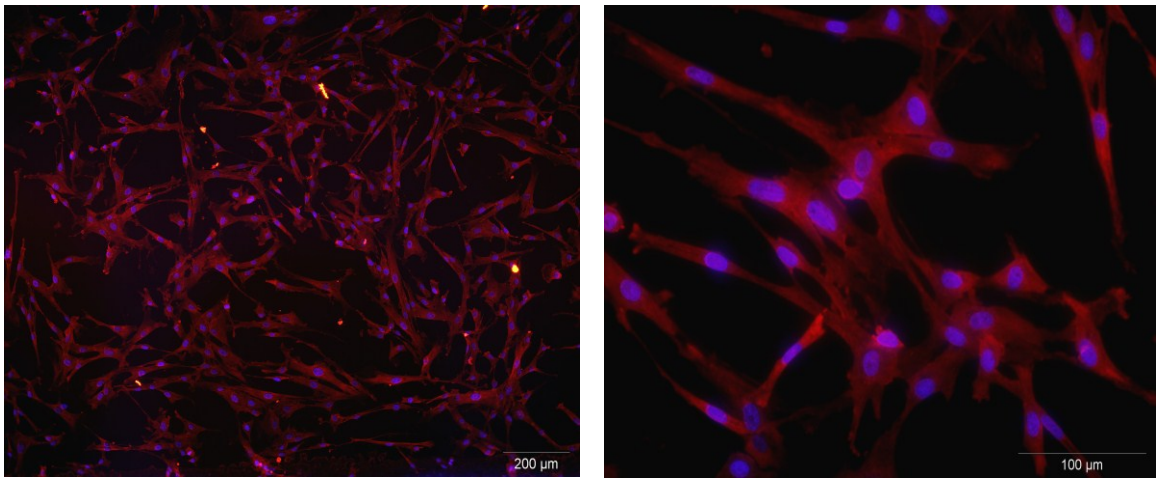

Fig. 2.1 Immunocytochemical staining for smooth muscle cells
At least 95% of cells alpha-actin stained positive in human pulmonary smooth muscle cells.

Cell treatment under normoxic and hypoxic conditions

The effect of hypoxia in the patch–clamp and calcium imaging studies was determined by switching between normoxic and hypoxic perfusate reservoirs. Normoxic solutions were equilibrated with 21% O_2 and 79% N_2. Hypoxic solutions were achieved by bubbling with 5% O_2 and 95% N_2 for at least 20 min prior to the cell perfusion. These procedures produced pO_2 of 140–160 mmHg (21% O_2) and 35–44 mmHg (5% O_2) values in the experimental chamber. O_2 levels were measured with a GemPremier3000 blood gas analyzer from samples directly taken from the experimental chamber containing the PASMCs during perfusion, which allows an exact measurement of pO_2. By the use of a small recording chamber (200 µl), high perfusion rate (2–3 ml/min), and short dead space, bath exchange could be achieved in <30s.

The hypoxic treatment of PASMCs (5% ambient oxygen) for phosphorylation studies (immuno-localization and immunoblots) were carried out in the XVIVO hypoxic work station from Biospherix (BioSpherix, Lacona, NY, USA) using fully-integrated incubators and the work station with dynamic programmable hypoxic and non-condensing humidity control at 37°C. Solutions used in these studies were equilibrated and kept in the hypoxic work station.

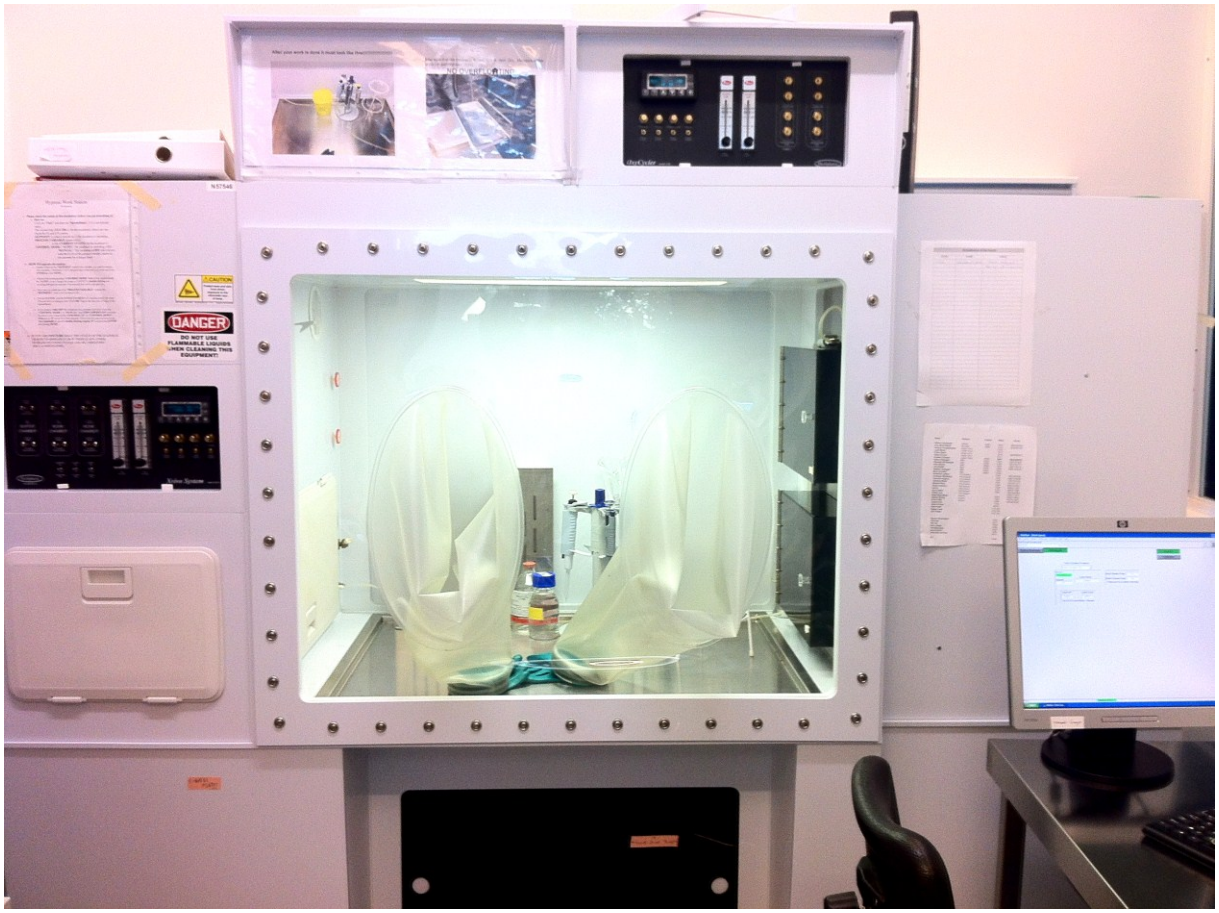

Fig. 2.2 Hypoxic work station

Fully-integrated incubators and work station with dynamic programmable hypoxic and non-condensing humidity control at 37°C was used in order to provide uninterrupted hypoxic conditions.

Isolated, perfused, and ventilated mouse lungs

Lungs of adult C57BL/6 mice (Harlan Laboratories, Inc) were removed from the chest under deep anesthesia, artificially ventilated and perfused with Krebs Henseleit buffer.

Mice were deeply anesthetized with isoflurane, if requiered supported with intraperitoneally administered medetomidin (0,25 mg/kg body weight) and ketamine (40 mg/kg body weight), and anticoagulated with heparin (1000 U/kg) by intravenous injection. Animals were then intubated via a tracheostoma and ventilated with a pre-mixed gas (21% O_2 5.3% CO_2, balanced with N_2; positive pressure ventilation, 250 µl tidal volume, 90 breath/min and 2 cmH_2O positive end-expiratory pressure). Midsternal thoracotomy was followed by insertion of catheters into the pulmonary artery and left atrium. Using a peristaltic pump

(ISM834A V2.10, Ismatec, Glattbrugg, Switzerland), buffer perfusion via the pulmonary artery was initiated at 37°C and a flow of 1 ml/min. Pressures in the pulmonary artery and the left atrium were registered via small diameter catheters (Hugo Sachs Elektronik, March-Hugstetten, Germany). During surgery, the lungs were ventilated with positive pressure. After placing the catheters, the artificial thorax was closed and the lungs were ventilated with negative pressure (VCM ventilator module/PLUGSYS device in combination with the artificial thorax type 839 (Hugo Sachs Elektronik, March-Hugstetten, Germany). For inspiration, negative pressure was adjusted to result in a tidal volume of ~ 250µl. End-expiratory pressure was held constant at −2 cmH_2O. A breath frequency of 90 per minute was used with 50% inspiration time. A deep inspiration was performed every 4 min with −20 cmH_2O.

Lungs included in to the study were those that had a homogeneous white appearance with no signs of hemostasis, edema or atelectasis. After an initial steady state period of 10 to 15 min, PP2 or PP3or dasatinib was added in to the buffer. In experiments with solvent (DMSO) the above agent was applied to the buffer in order to check, whether the solvent had any influence on the pulmonary artery pressure. Delta PAP indicates the pulmonary arterial pressure after application of PP2 or PP3 or Dasatinib at a chosen concentration minus the pulmonary arterial pressure before.

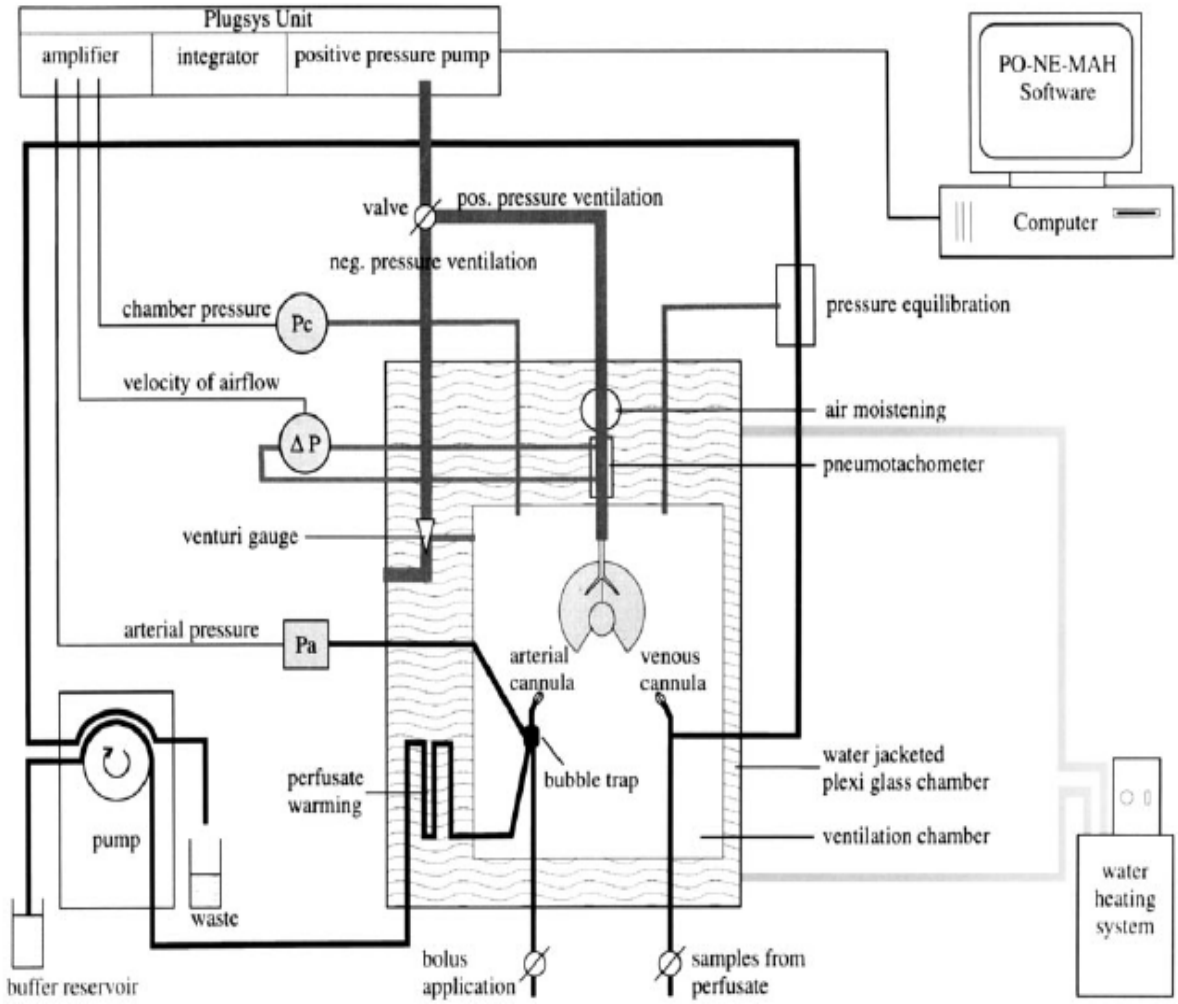

Fig 2.3Scheme of the isolated perfused mouse lung

The perfusion system is drawn in black, the ventilation system in gray. The water circulation system is marked by black waves. From (Bethmann *et al.*, 1998)

Isolation of RNA and cDNA synthesis

RNA was extracted from cells using spin-columns (RNeasy, Qiagen, Germany). For reverse transcription (RT) of extracted RNA, 1 µg of total RNA in a total volume of 10µl was mixed with 1µl of dNTP and 1µl of random hexamers and denatured at 75 °C for 3 min. After cooling on ice, the following components were added to the samples: 4 µl of 5X RT buffer, 2 µl of 0.1 M dithiothreitol, 1µl of RNAse inhibitor (Peqlab, Erlangen, Germany) and 1 µl Moloney murine leukemia virus reverse transcriptase (MMLV,Invitrogen) and then incubated at 25°C for 10 min and 37°C for 1h.

Agarose gel electrophoresis

DNA samples were mixed with loading buffer and loaded onto a 2% agarose gel. The electrophoresis was performed for approx 1 hour with 100 volt. The negatively charged DNA migrated from the cathode (-) to the anode (+). To visualize the DNA, the gel was treated with ethidium bromide that intercalates into the DNA double strands forming a fluorescent complex by excitation under UV light. DNA bands were detected by chemiluminiscence imager. The size of DNA fragments was determined by comparison with a DNA size marker.

Buffers used in agarose gel electrophoresis:

10x TAE buffer for agarose gels: 0.4 M Tris, 0.4 M acetic acid, 10 mM EDTA (pH adjusted with HCl to 8.0). Agarose gel (1%): 10% of 10x TAE, 1% of agarose, 0.5 µg/ml of ethidium bromide. DNA loading buffer: 0.01% of bromophenol blue, 40% of glycerol, 10% of 10x TAE buffer.

RT-PCR

For reverse transcription (RT) of extracted RNA, 1 µg of total RNA was mixed with 1 µl of random hexamer primer and the reaction volume was made up to 11.5 µl adding DEPC-treated water (reaction mixture) , then by heated at 65°C for 5 min, and chilled in ice. Reaction buffer of 4µl for reverse transcriptase, RiboLock™0.5 µl. RNase Inhibitor, 2 µl of dNTP Mix and 1 µl RevertAid™ H Minus Reverse Transcriptase were added to the reaction mixture. The final reaction mixture was incubated for 10 min at 25°C, followed by 60 min at 42°C and the reaction was terminated by heating at 70°C for 10 min. The reverse transcription reaction product was directly used in the PCR reaction or stored at -20°C.

PCR

For PCR 1 µl of 10 pM forward primer, 1 µl of 10 pM reverse primer, 100 ng of cDNA and 12.5 µl of AmpliTaq Gold® 360 Master Mix were added then final reaction mixture and the reaction volume was increased to 50 µl addition of Double distilled water. The thermal cycler protocol consisted of an initial incubation at 95°C for 5 min, followed by 30 cycles at 95°C for 30 s, 60°C for 30 s and 72°C for 60 s, and a final extension at 72°C for 10 min. Sequences of primers used in RT PCR are listed in Table 2. The final PCR product was loaded in 1% agarose gel and ethidium bromide was used for the visualization of the product along with the molecular weight marker.

Quantitative RT-PCR

Real-time PCR was used for relative quantification of the C-Src and Fyn mRNA, GAPDH was used as the reference gene .The reactions were performed in an ABI 7700 Sequence Detection System (Applied Biosystems, Foster City, CA) using the SYBR-Green method in 10 µl reactions containing cDNA samples, 1x Mastermix for SYBR Green forward and reverse primer. The amplification protocol was 1× (50°C, 2 min); 1× (95°C, 6 min); 45× (95°C, 5s; 60°C, 5s; 73°C, 10s). The data for the amplification curves were acquired after the extension phase at 73°C. After amplification, melting curves were analyzed for the fluorescence signal. Each gene was measured in triplicate in three independent experiments. The Δct values for each target gene were calculated for reference genes using the averaged ct values by the formula Δct = ct(reference) – ct(target) and silencing was expressed as percentage.

Table 2. Primers used for real-time PCR

Target gene	Sequence 5' → 3'
c-Src	**GGGTAGCAACAAGAGCAAGC** **GAGTTGAAGCCTCCGAACAG**
Fgr	**GGACTGCAGGTACTCGAAGG** **AACTACATTCACCGCGACCT**
Yes	**TATGGCTGCTCAGATTGCTG** **TTCAGGAGCTGTCCATTTGA**
Lyn	**TGTGAGAGATCCAACGTCCA** **TTTGCTTTCCACCATTCTCC**
Fyn	**TGAACAGCTCGGAAGGAGAT** **GGTTTCACTCTCGCGGATAA**
Lck	**CTTCCCCACTGCAAGACAAC** **GCCACCGTTGTCCAGATTAC**
TASK-1	**CGGCAAGGTGTTCTGCATG** **CAAGGTGTTGATGCGCTCG**
GAPDH	**CGTCATGGGTGTGAACCATG** **GCTAAGCAGTTGGTGGTGCAG**

Annealing of siRNA

RNA oligonucleotides were dissolved at a convenient concentration, e.g. 100 µM, in RNAse free water and stored at –20°C. RNA oligonucleotide were given to the annealing buffer to a final concentration of 50 µM Combining 30 µl of each RNA oligonucleotide (sense and antisense oligonucleotide) and 15 µl of annealing buffer. results in final volume is 75 µl, and a final siRNA duplex concentration of 20 µM.

The solution was incubated for 1 minute at 90°C cooled down to room temperature over a period of 45 min and stored at 4°C or on ice until ready to use.

Annealed siRNA can be safely stored frozen at –20°C

Annealing buffer ingredients:

30 mM HEPES-KOH pH 7.4, 100 mM KCl, 2 mM MgCl2, 50 mM NH4Ac

Transfection of hPASMC with small interfering RNA against C-Src, Fyn, and TASK-1

Small interfering RNAs (siRNA) against C-Src (siC-Src), Fyn (siFyn) and Task-1 (siTASK-1) were commercially synthesized (Eurogentec, Seraing, Belgium). As negative control, non silencing RNA (nsRNA), which does not target any human gene product, was used. The hPASMCs were grown on coverslips or in 6-well plates, to which annealed siRNA was transfected using Effectene transfection reagent (QIAGEN). Gene knock-down was checked by quantitative RT-PCR using the RNA extract (RNeasy, QIAGEN) and at the protein level by Western blots from the transfected cells.

RNA levels, live cell calcium and electrophysiological measurements were performed 48–56h post transfection. To assess the efficiency of the siRNA-transfection FITC-conjugated siRNA were used. Only FITC-positive cells were taken for the electrophysiological studies. In addition, TASK-1-siRNA-transfection was functionally controlled by superfusion of the cells with a bath solution adjusted to pH of 8.3.

Table 3. Sequence of siRNA used for the silencing the specific gene product as listed

TASK-1	**UCACCGUCAUCACCACCAUdTdT** **AGUGGCAGUAGUGGUGGUAdTdT**
C-Src	**UUCGGAGGCUUCAACUCCUdTdT** **AGGAGUUGAAGCCUCCGAAdTdT**
Fyn	**AGAUGCUGAGCGACAGCUAdTdT** **UAGCUGUCGCUCAGCAUCUdTdT**
Non silencing	**AGGUAGUGUAAUCGCCUUGdT dT** **CAAGGCGAUUACACUACCUdTdT**

Protein concentration measurement

The BCA protein assay kit (Thermo Scientific, Pierce Biotechnology) was used as measurement of the protein concentration. This method is based on peptide bonds mediated reduction of Cu^{2+} to Cu^{1+} that interacts with bicinchoninic acid (BCA) generating a purple-colored product and it is useful for the measurement of protein concentrations in buffers containing various chemical agents including SDS and Tx-100. Dissolved samples (in 1x Laemmli sample buffer and buffer containing 1% of Tx-100) were directly applicable for the protein concentration measurement. Preparation of standards (differently diluted bovine serum albumin); incubation conditions, spectrophotometric measurement and calculation of protein concentration were performed according to the instruction from the company. The absorbance of the purple color product was measured on a 96 well plate at 492nm with a spectrofluorometer (FL-600). As background, absorbances of relevant buffer(s) were used.

Immunoblotting

Protein extracts of hPASMCs were prepared in RIPA buffer containing the protease-inhibitor and phosphatase-inhibitor tablet (Roche, Vienna, Austria). Equivalent amounts of protein were resolved on 10% SDS polyacrylamide gels and then proteins transferred to the nitrocellulose membrane. Nonspecific antibody binding was blocked by incubation in 5% (m/v) non-fat dry milk powder in TBST (20 mM Tris-Cl, pH 7.5, 150 mM NaCl, 0.1% (v/v) Tween 20) at room temperature for 1 h. then, samples were incubated overnight in a 1:1000 diluted primary antibody solution at 4°C. After washing the membranes in TBST buffer and incubating them in asolution of with 1:2000 diluted horseradish-peroxidase conjugated anti-IgG secondary antibody for 1 h at room temperature, specific immunoreactive signals were detected by enhanced chemiluminescence (ECL, Amersham, Freiburg, Germany). Anti-src, anti-phospho-src, and anti-nonphospho-src antibodies were obtained from Cell Signalling Technology Inc.

Immunofluorescence staining

Immunofluorescence was performed using smooth muscle cell alpha actins, myosin heavy chain-7 antibodies and von Willebrand factor. hPASMCs grown on glass slides were fixed for 5 minutes in cold methanol,and rinsed 5 times in PBS. After blocking with 1% BSA overnight, cells were incubated with the anti-alpha actin antibody, myosin heavy chain-7 antibodies and von Willebrand factor antibodies (1:50 dilution) for 1 hrs and then probed for 40 minutes with the fluorescent labelled secondary antibodies (anti-goat IgG-FITC or anti-rabbit Alexa 555). Cells were counterstained with DAPI to identify the nuclear DNA. Duplicates were processed without primary antibodies as controls. Fluorescence was imaged with a [Leica DM2500 M microscope, using Leica 40x (N.A. 1.0) objective].

Immuno co-localization

hPASMCs grown on glass slides were treated in SMC medium at 37°C under either normoxic or hypoxic (5% O_2) conditions for 15 minutes. Reactions were stopped additing of 4% paraformaldehyde in PBS for 20 min. Fixed cells were permeabilized with 0.1% BSA,and 0.5% Triton-X100 in PBS for 30 min, then rinsed five times in PBS followed by blocking them with 3% BSA in PBS for 1 h. Then the cells were stained overnight with mouse anti-src (1:100) or mouse anti-phospho-src (1:100) or mouse anti-non-phospho-src (1:100) and rabbit anti-TASK-1 primary antibody (1:100) at 4°C followed by incubation with anti-rabbit Alexa Fluor 488-labelled secondary antibody (1:500) and anti mouse Alexa Fluor 596 (1:500) for 1 h at room temperature. Cells were counterstained with DAPI to identify nuclear DNA. Duplicates were processed without primary antibodies for controls. Analysis of the staining was made with a confocal laser scanning microscope (LSM Zeiss Axiovert 200M). Images were taken with x60 oil immersion objective with 1.4 N/A.

Immunoprecipitation for TASK-1

PASMC lysates (100 µg) were prepared in IP Buffer {20 mM Tris-HCl, 100 mM NaCl, 1% Triton X-100, 0,1% SDS, 2 mM EDTA, 1 mM PMSF, 1 mM sodium orthovanadate, 1x protease inhibitor coctail (Roche)} and incubated overnight at 4°C with 1 µl (1ug/ml) of rabbit anti-TASK-1 antibody (Abcam) or IgG as an isotype control (R & D Systems). Samples were transferred to tubes containing 50 µl protein A-Sepharose^{TM} CL-4B beads (Amersham Biosciences). After 1 h of incubation at 4°C, immunoprecipitates were washed several times with IP, boiled in SDS sample buffer, separated by SDS-PAGE under reducing conditions, and transferred to a polyvinylidene difluoride membrane. Immunoblots were analyzed using rabbit anti-TASK-1 (Abcam) mouse anti-phospho-tyrosine antibodies (Millipore) and C-Src (Cell Signalling).

Electrophysiology

Whole-cell patch-clamp technique on hPASMC was used as previously described to measure the resting membrane potential under current clamp and macroscopic potassium (K^+) currents under voltage clamp(Olschewski *et al.*, 2006, Li *et al.*, 2012).Cells were superfused at room temperature in bath solution (see. Solutions) For TASK-1 recording, pipettes were filled with Pipette solution 1 (see. Solutions). The non-inactivating TASK-1 K^+ current (IKN) was obtained from the holding potential of 0 mV by stepping the voltage to 60 mV and then ramping it to -100 mV over a period of 1.6 seconds. To isolate the non-inactivating TASK-1 K^+ current (IKN) from other voltage-dependent K^+ currents, cells were clamped at 0 mV for at least 5 min as previously described. As we have already shown, under these conditions TEA, ITX or 4-AP have no significant effect on ITASK-1. For the recording of calcium-activated K^+ channels (KCa) and whole cell K^+ current, the same bath solution was used and the pipette solution was the Pipette solution 2(see.solutions). The free intracellular calcium concentration [Ca^{2+}] was 900nM, which promotes KCa channel activation. The KCa currents were obtained under whole-cell patch-clamp conditions, from a holding potential of –20 mV, with 10 mV depolarizing pulses lasting 400 ms, to +50 mV. The whole cell K^+ current was obtained under whole-cell patch-clamp conditions, from a holding potential of –80 mV, with 10 mV depolarizing pulses lasting 400 ms, to +50 mV. Pipettes pulled from borosilicate glass tubes (GC 150, Clark Electromedical Instruments, Pangbourne, UK) were fabricated on a P-97 electrode puller (Sutter Instruments, Novato, CA, USA) and fire-polished to give a final resistance of 2 – 3 MΩ for whole-cell recording. The effective corner frequency of the low-pass filter was 0.5-5 kHz. The frequency of digitization was at least twice that of the filter. No

leak subtraction was made. The data were stored and analyzed with commercially available pCLAMP 9.0 software (Axon Instruments, Foster City, CA, USA).

Measurement of the intracellular calcium concentration ($[Ca^{2+}]_i$)

The cells were cultured on glass coverslips until confluency and loaded in the dark for 30 min with the fluorescent dye fluo-4-AM (2 μM) followed by a washing step with 1.8 mmol/L Ca^{2+} containing bath solution. After 15 min, a single glass coverslip was mounted on the stage of a Zeiss 200M inverted epifluorescence microscope coupled to a PolyChrome V monochromator (Till Photonics, Germany) light source in a sealed, temperature-controlled RC-21B imaging chamber (Warner Instruments, USA) and perfused with bath solution. Fluorescence images were obtained with excitation at 490 nm. The emitted light was collected at 516 nm by an air cooled Andor Ixon camera. Measurements were made every 3s. Background fluorescence was recorded from each cover slide and subtracted before calculation. The fluorescence value of the last 30 measurement points (90 s) prior to application of hypoxia were averaged and considered as baseline value. This value has been subtracted from the maximum fluorescence value providing the peak calcium response in fluorescence. Each individual raw graph was normalized to its baseline value. The acquired images were stored and subsequently processed offline with TillVision software (Till Photonics, Germany).

Solutions

Bath solution (in mmol/L): NaCl 130, KCl 5.5, $CaCl_2$ 1.5, $MgCl_2$ 1, glucose 10, Na_2HPO_4 0.5, KH_2PO_4 0.5, HEPES 10; adjusted to pH 7.3 with NaOH.

Pipette solution 1 for KCa recording (in mmol/L): KCl 20, K-methanesulphonate (to suppress Cl- currents) 115, $MgCl_2$ 1, $CaCl_2$ 2, Na_2ATP 2, ethyleneglycol bis(ß-aminoethyl ether)-N,N,N',N'-tetraacetic acid (EGTA) 3, HEPES 10; pH adjusted to 7.2 with KOH. The free [Ca^{2+}], calculated with Maxchelator (http://www.stanford.edu/%7Ecpatton/maxc.html), was 900 nM. The pipette solution with K-methanesulphonate added to suppress Cl- currents.

Pipette solution 2 for TASK recording (in mmol/L): KCl 20, K-methanesulphonate 115, $MgCl_2$ 1, Na_2ATP 2, EGTA 3, HEPES 10; pH adjusted to 7.2 with KOH. The free [Ca^{2+}] was around 0 nM.

Physiological salt solution (PSS in mmol/L): NaCl 118, $NaHCO_3$ 24, $MgSO_4$ 1, NaH_2PO_4 0.435, glucose 5.56, $CaCl_2$ 1.8, and KCl 4.

Physiological balances solution (in mmol/L): NaCl 118, $NaHCO_3$ 24, $MgSO_4$ 1, NaH_2PO_4 0.435, glucose 5.56, $CaCl_2$ 1.8, and KCl 4.

Krebs Henseleit buffer (mmol(L): NaCl 120, KCl 4.3, KH_2PO_4 1.1, $CaCl_2$ 2.4, $MgCl_2$ 1.3, and glucose 13.32, as well as 5% [wt/vol] hydroxyethylamylopectin [molecular weight 200,000]. $NaHCO_3$ was adjusted to result in a constant pH of 7.37 - 7.40.

Chemicals

Chemicals are listed in Table.4. Application of the vehicle alone at a maximal concentration (1:1,000 dilution of DMSO or ethanol in Ringer bath solution) did not have any effect on either K^+ current or resting membrane potential. The pH value of drugs containing solutions was tested and corrected to eliminate potential pH-induced effects. These drugs were diluted with bath solution to the appropriate concentration on the day of the experiment.

Table.4. Chemicals and toxins

Chemical	Company	Concentration	Usage	Diluted in
PP2 (4-Amino-5-(4-chlorophenyl)-7-(t-butyl)pyrazolo[3,4-d]pyrimidine)	Sigma	10nM	C-Src inhibitor	DMSO
PP3 (4-Amino-7-phenylpyrazol[3,4-d]pyrimidine)	Sigma	10nM	inactiveC-Src inhibitor	DMSO
4-AP	Sigma	0.1mM	K_V blocker	Ringer
Anadamide	Sigma	10μM	TASK-1 blocker	Ethanol
Iberitoxin	Sigma	50 nM	K_{Ca} blocker	Ringer without Ca^{2+}
Src Activator peptide	Santa Cruz			DMSO
Dasatinib	enzo	100		DMSO
RT-PCR	Fermentas			
PCR	Applied Biosystems			
qPCR	Qiagen			

Statistical analysis

Numerical values are given as means ± SE of n cells or measurements. Intergroup differences were assessed by a factorial analysis of variance with post-hoc analysis with Tukeys significant difference test, or Student's unpaired and paired t-tests as appropriate. p values <0.05 were considered significant and shown as * in the figures (*<0.05, **<0.01; ***<0.001 compared to control).

Results

Results

Modulation of TASK-1 channels by G protein-coupled pathways

Modified from

Tang B., Li Y., **Nagaraj C**., Morty RE, Gabor S., Stacher E., Voswinckel R., Weissmann N., Leithner K., Olschewski H., Olschewski A.: Endothelin-1 Inhibits Background Two-Pore Domain Channel TASK-1 in Primary Human Pulmonary Artery Smooth Muscle Cells. Am J Respir Cell Mol Biol Vol 41. pp 476–483, 2009

Endothelin (ET)-1 is considered to be a major player within the pathologic mechanisms involved in pulmonary arterial hypertension (PAH) Endothelin-1 acts via the G-protein coupled receptors ET-A or ET-B, and specific antagonists of ET-1 receptors represent an important pillar of modern therapy of this devastating We found that ET-1 inhibits TASK-1 dose-dependently in human PASMC through the Gαq-receptor ET_A. To further assess the mechanism involved in ET-1–induced TASK-1 inhibition, hPASMCs were incubated for 10 minutes in ET-1 (10 nM). No differences in the tyrosine phosphorylation of TASK-1 was observed when comparing ET-treated and untreated groups were compared (n = 3; Figure 3.2). In contrast, the incubation with ET-1 stimulated the threonine phosphorylation of TASK-1, as was evident in TASK-1 immunoprecipitates probed with an anti-phosphothreonine antibody (Figure 3.1). Protein loading equivalence was demonstrated by probing immunoprecipitates with an anti–TASK-1 antibody (Figure 1).

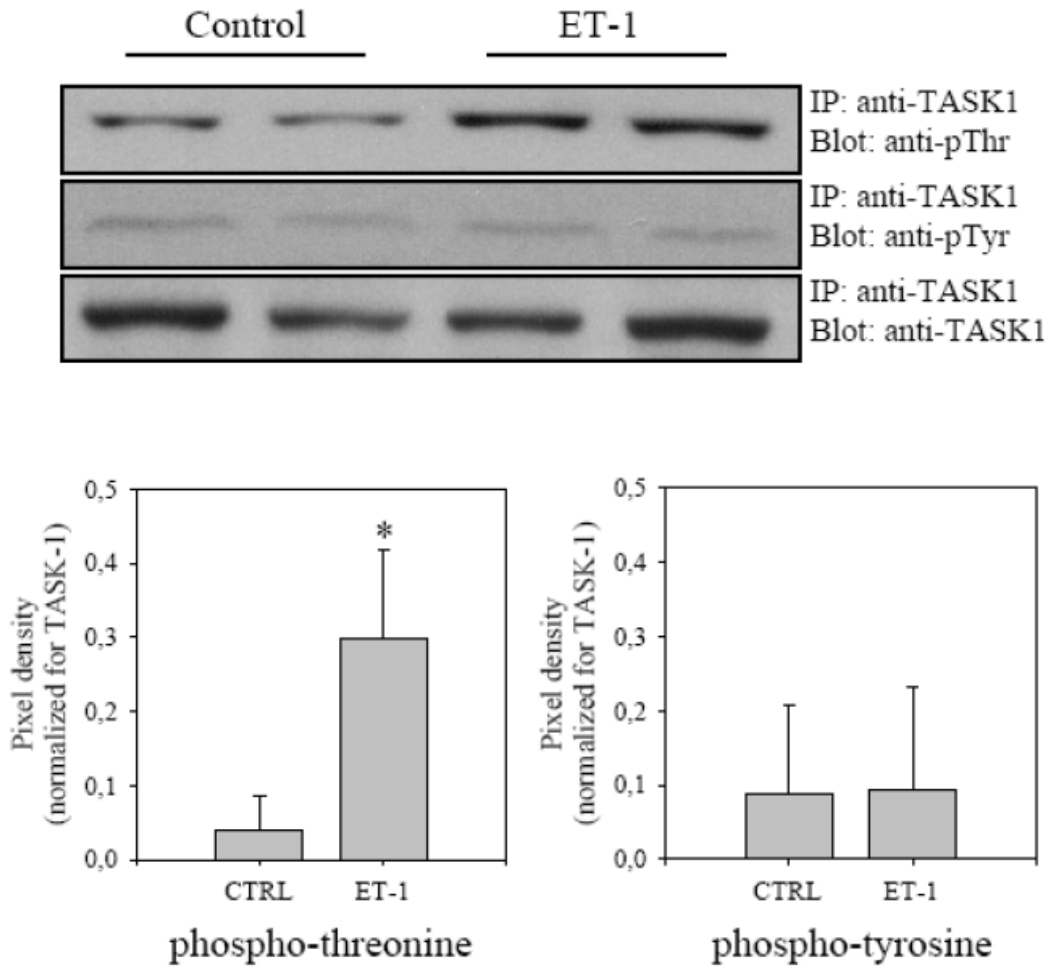

Figure 3.1. PKC-dependent phosphorylation of TASK-1 by ET-1.

Representative results of the threonine (left) and tyrosine (right) phosphorylation of TASK-1 in ET-1-treated and untreated (control) hPASMCs. Protein loading equivalence is shown by probing immunoprecipitates with an anti-TASK-1 antibody in the lower panel.

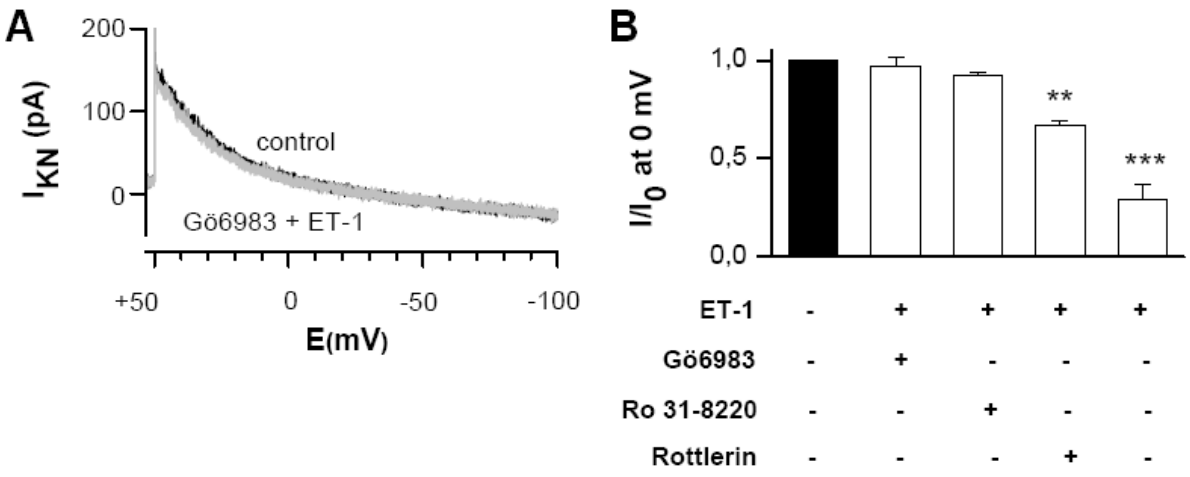

Figure 3.2. Impacts of PKC inhibitors on the ET-1 effect.

(**A**) Representative traces show the lack of ET- 1 (10nM) effect on TASK-1 after 1 h preincubation with Gö6983 (10 nM). (**B**) The histogram summarizing the effect of ET-1 on the TASK-1 current after pretreatment of hPASMCs with Ro318220 (1μM), Gö6983 or rottlerin (10 nM) (n = 6 each group; **, $p < 0.01$; ***, $p < 0.001$ difference from ET-1-untreated cells). I/I_0 is the current in the presence of ET-1 expressed as a fraction of the current prior to ET-1 application.

Modulation of TASK-1 channel by hypoxia

Modified from

Nagaraj C, Tang B, Bálint Z, Wygrecka M, Hrzenjak A, Kwapiszewska G, Stacher E, Lindenmann J, Weir EK, Olschewski H, Olschewski A.: Src tyrosine kinase is crucial for potassium channel function in human pulmonary arteries. *Eur Respir J.* 2012 Apr 20

Expression of SrcTK in human lung and PASMC

To analyze the expression of SrcTK isoforms, C-Src, Lck, Lyn, Fyn, Yes, and Frg, we performed RT-PCR on human lung tissue, human pulmonary artery and human pulmonary artery smooth muscle cells (hPASMCs) (Figure 3.3). Our results demonstrated the presence of mRNA encoding all investigated isoforms in lung tissue. Human primary PASMCs expressed mRNA only for the isoforms C-Src, Fyn and Yes. We obtained identical results with at least 3 preparations of RNA from different donor lungs and primary hPASMCs.

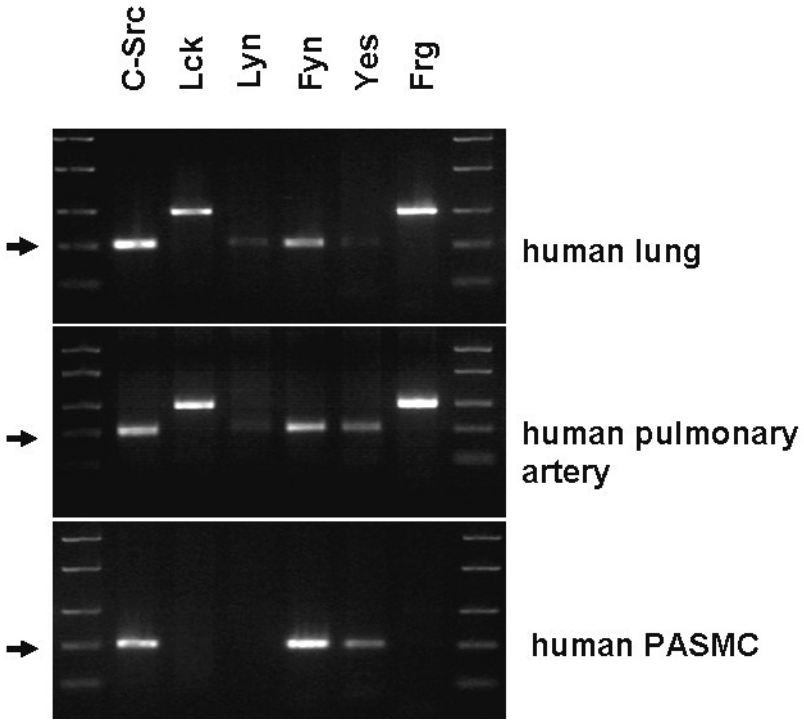

Figure 3.3. Expression of of SrcTK isoforms in primary hPASMC.

RT-PCR screening for SrcTK in RNA extracts of homogenized human lung tissue and human primary PASMC. Representative gels illustrate mRNA expression of c-Src (204 bp), Lck (398 bp), Lyn (213 bp), Fyn (206 bp), Yes (202 bp) and Frg (402 bp). The arrows indicate 200 bp.

SrcTK interacts with TASK-1 channels in hPASMC

As our group has previously shown, the background K^+ channel TASK-1 controls the resting membrane potential and thus the human pulmonary smooth muscle cell tone(Gurney *et al.*, 2002, Gurney and Manoury, 2009) (Olschewski et al, Circ res 2006). Next we investigated the interaction of SrcTK and TASK-1 channels. C-SrcTK is targeted to the plasma membrane due to a myristylated N-terminal region. The SH1 domain of the SrcTK contains the phosphorylation site tyr419 which is required for full C-SrcTK activation(Kim *et al.*, 2009)(Holmes *et al.*, 1996). This mechanism allows C-SrcTK to interact with ion channels to modulate their properties(Holmes *et al.*, 1996). The C-terminus of the background TASK-1 potassium (K^+) channel contains possible phosphorylation sites for tyrosine and serine kinases (Figure 3.4).

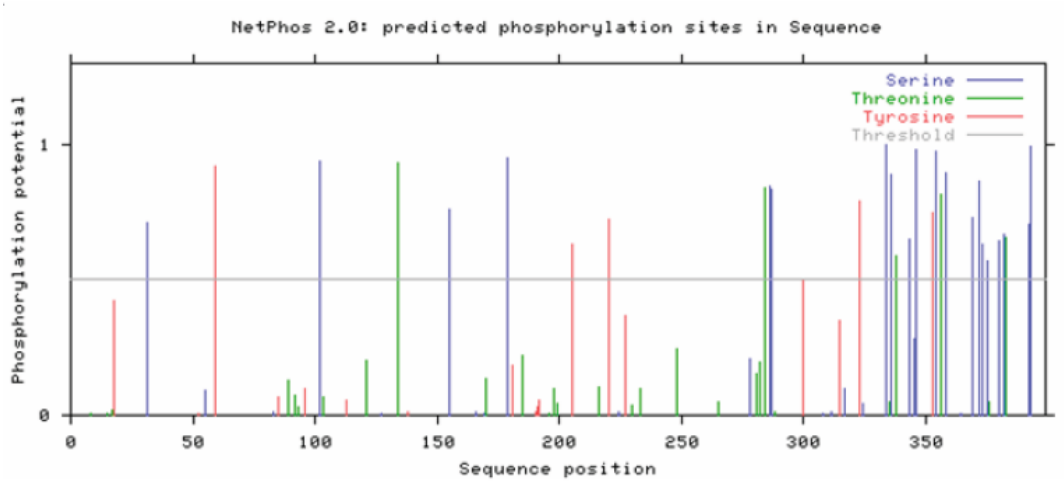

Figure 3.4. Predicted phosphorylation sites in human TASK-1

In order to elucidate the interaction of SrcTK and TASK-1 channels, we performed co-immunoprecipitation studies. Immunoprecipitation (IP) was performed with an anti- SrcTK antibody or isotype control (IgG) of the hPASMC lysate. With the precipitated samples later immuno blot was performed (IB) with anti- TASK-1 (top panel) TASK-1 precipitated along

with SrcTK (Figure 3.5). blotting for SrcTK (bottom panel) resulting in a single band for SrcTK along with heavy chain.

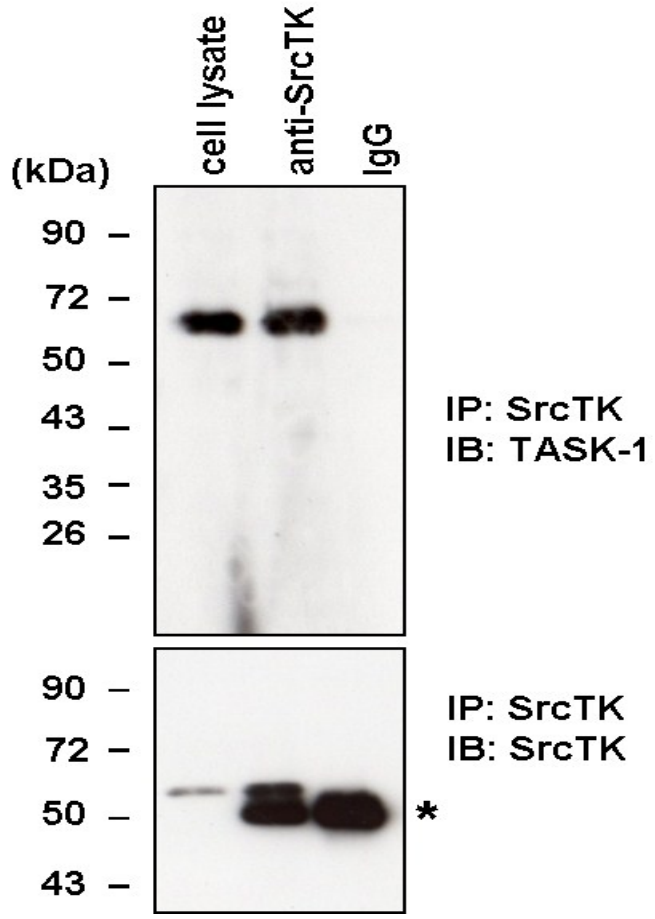

Figure3.5. Interaction of SrcTK and TASK-1 in primary hPASMC. The blots represented here show co-immunoprecipitation performed with anti-SrcTK and TASK-1. Isotype contol IgG and cell lysate, then immunoblotted for TASK-1(upper panel) and SrcTK (lower panel). Star indicates IgG.

SrcTK is co-localized with TASK-1 channels in hPASMC

The antibodies for TASK-1 and SrcTK used in co-localization study were evaluated by immunoblot, which show a single band without any unspecific back ground (Figure 3.6A). The localization of the background TASK-1 channel and SrcTK were examined in hPASMC and visualized by confocal laser scanning microscopy. Immunofluorescent staining of TASK-1 and SrcTK revealed that TASK-1 and SrcTK are co-localized in the cell membrane (Figure 3.6B). Staining was absent in negative controls, when we imaged cells without exposure to primary antibody used as negative controls.

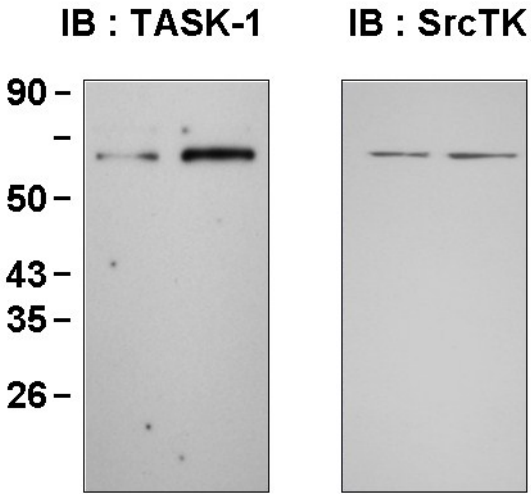

A

B

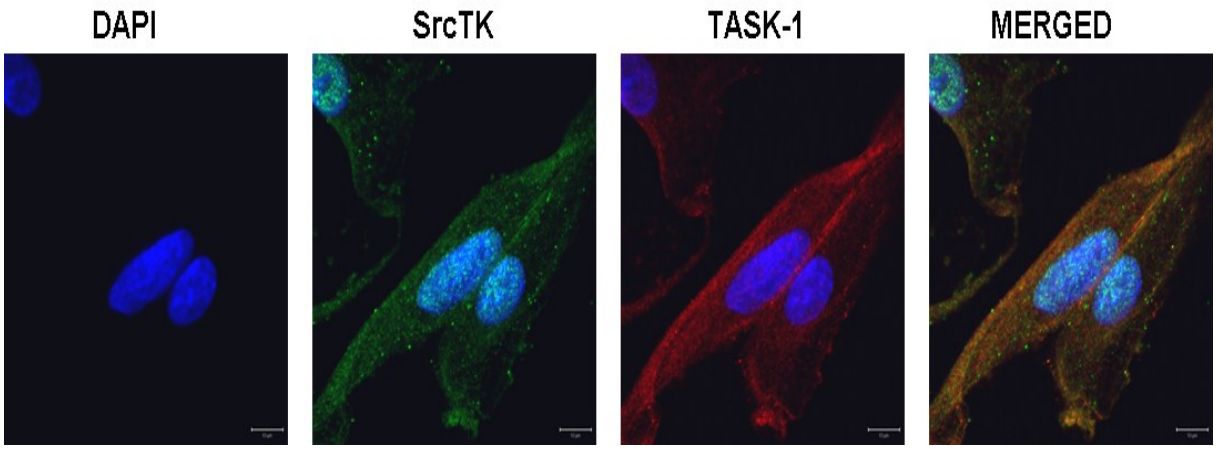

Figure 3.6. Co-localisation of SrcTK and TASK-1 in primary hPASMC.

(A) Immunoblot of TASK-1 and SrcTK from cell lysate of hPASMCs is presented. **(B)** Fluorescent double-immunostainings indicate DAPI nuclear staining (blue), Src family kinases (red), TASK-1 channel (green) and merged (yellow).

SrcTK modulates TASK-1 channel activity in hPASMCs

To further confirm the functional relevance of the SrcTK interaction with TASK-1 channels, we used pharmacological tools and siRNA techniques. Patch-clamp recordings of the non-inactivating TASK-1 current (I_{KN}) on hPASMCs were made as described previously in the methods chapter in detail. We detected that SrcTK controls TASK-1 channel activity as confirmed by silencing of C-Src and Fyn in primary hPASMCs, resulting in a decreased current compared to control (Fig. 3.7A and 3.7B). TASK-1 current density was significantly inhibited by treatments with the SrcTK inhibitor PP2 (0.2383±0.6 pA/pF; n=12) or transfection with siC-Src (0.172±0.1 pA/pF; n=4) or siFyn (0.205±0.02 pA/pF; n=8) compared to control (0.668±0.1 pA/pF; n=13). The treatment with PP3 (0.582±0.2 pA/pF; n=4) or transfection with non-silencing(ns)RNA (0.620±0.02 pA/pF; n=8) did not affect the TASK-1 current (Fig. 3.7C).

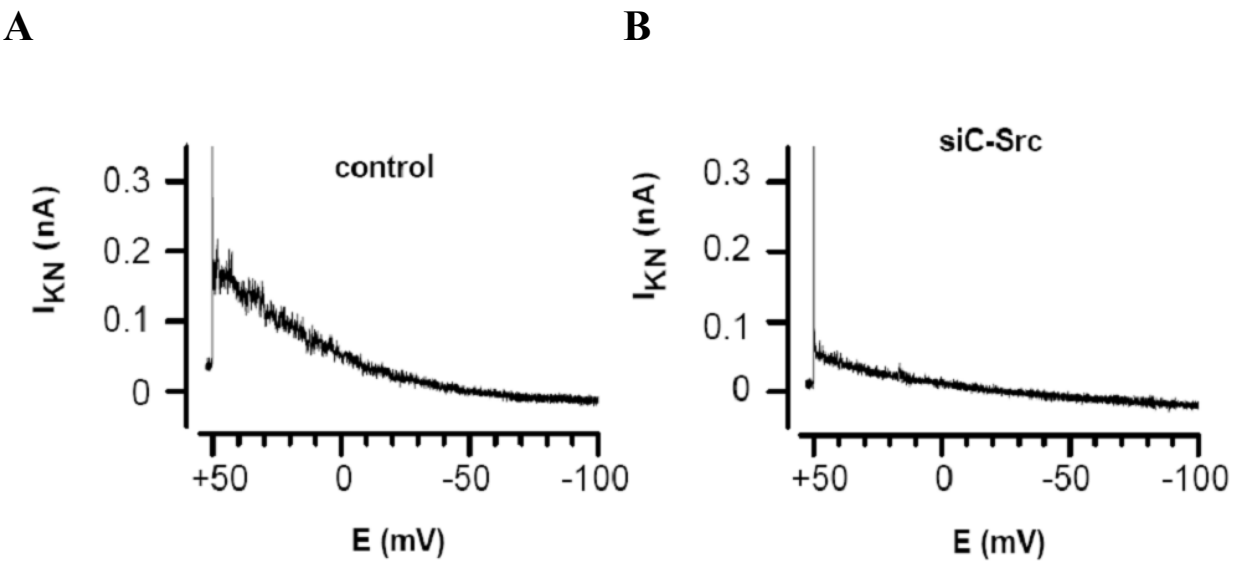

C

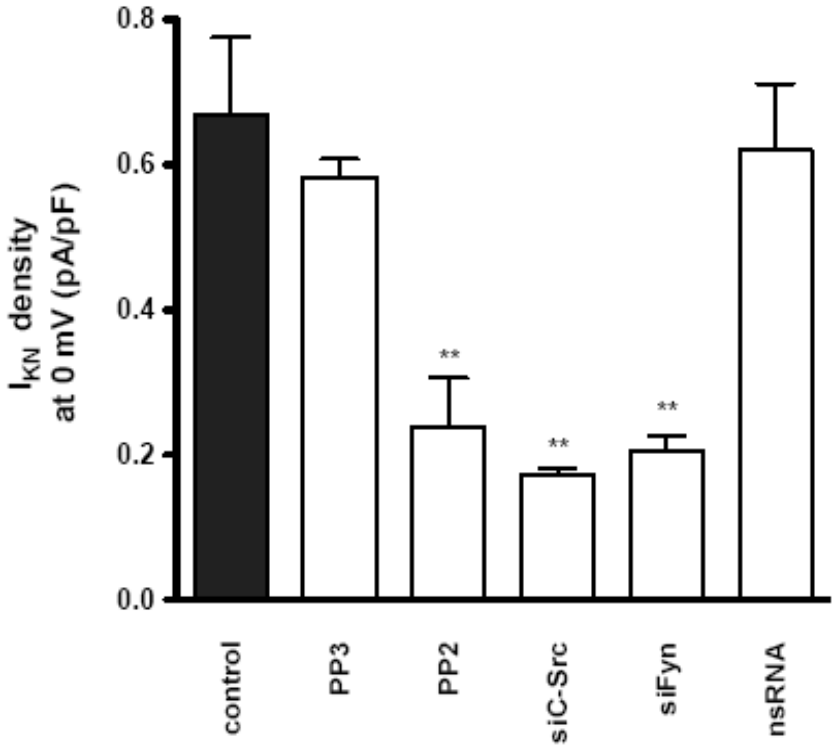

Figure 3.7. SrcTK is crucial for TASK-1 channel activity in primary hPASMC. (A) Representative recordings of TASK-1 current (I_{KN}) are shown in control cells. **(B)** Original recordings of TASK-1 in cells transfected with siC-Src. **(C) The** histogram summarizes the TASK-1 current density in primary hPASMC. After treatment with Src family kinase inhibitor PP2 (1 μM) or transfection with siC-Src and siFyn, the current density was significantly reduced. We did not detect any significant reduction of current density after transfection with non-silencing (ns)RNA or after treatment with PP3 (1 μM; inactive analog of PP2).

TASK-1 channels can be modulated by different pathways, such as AMPK, PKA, PKC and PLC, in response to different agonist stimulations. In order to exclude the involvement of these pathways, we investigated the hypoxic inhibition of TASK-1 current

using different inhibitors. None of these treatments affected the control TASK-1 current or its hypoxic inhibition showing that AMPK, PKA, PKC and PLC are not involved (Figure 3.8).

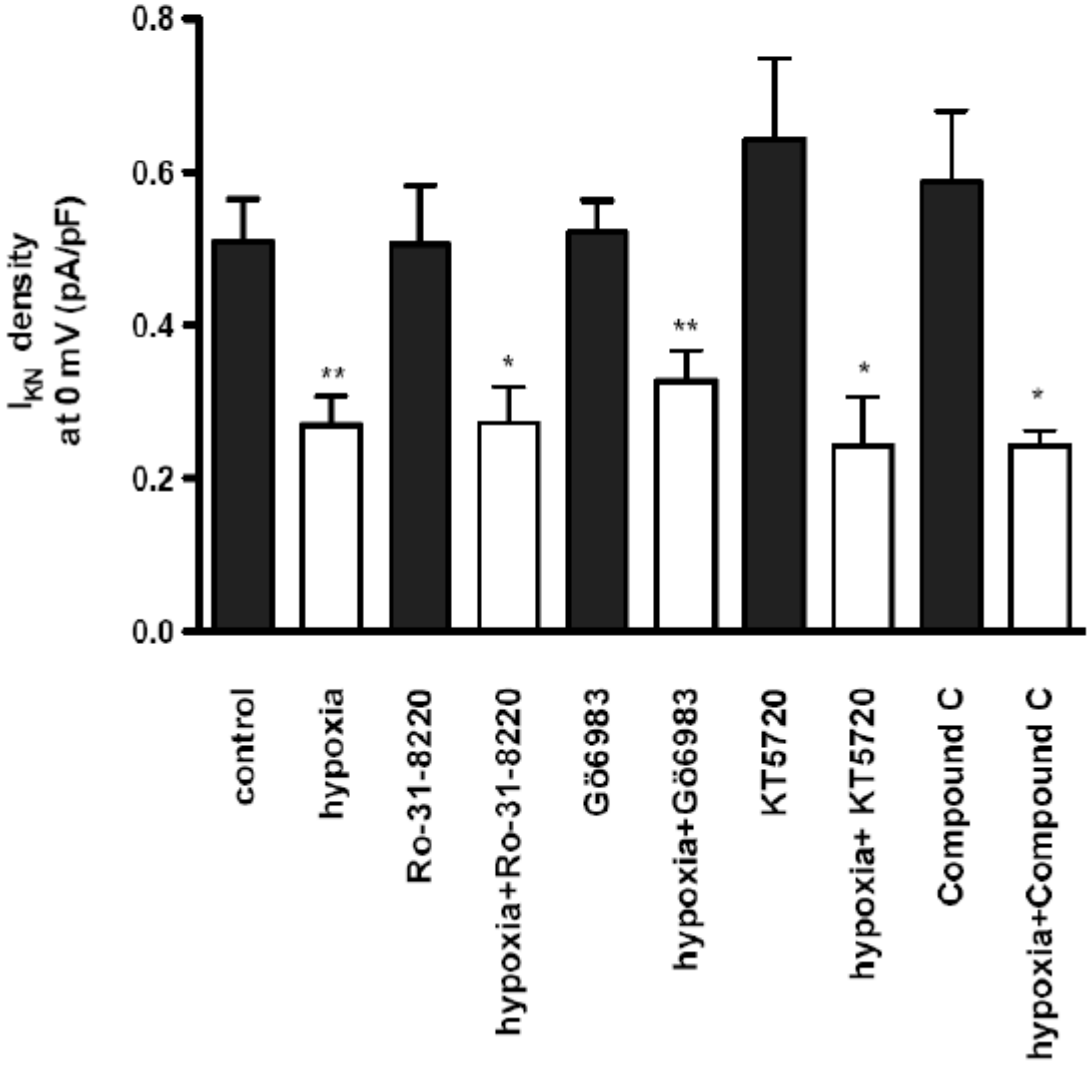

Figure 3.8. Lack of the effect of AMPK, PKA, PKC and PLC inhibition on the hypoxia-sensitivity of TASK-1. Bar graphs shows the I_{KN} density of TASK-1 channel in the presence of Ro-31-8220 (PKC inhibitor), Gö6983 (PKC inhibitor), KT5720 (PKA inhibitor), and compound C (AMP-activated kinase inhibitor) under normoxia (control) and hypoxia in primary hPASMCs (supported by Bi Tang, MD PhD).

SrcTK inhibition depolarizes hPASMCs

TASK-1 channels are active at resting membrane potential and set the negative resting membrane potential in PASMCs, as we have previously demonstrated by siRNA treatment in primary human PASMCs. As the SrcTK inhibition also decreases the TASK-1 current (Fig. 3.9), we further investigated the physiological role of SrcTK for the resting membrane potential of primary hPASMCs by means of patch-clamp. Electrophysiological measurements carried out in hPASMCs showed a significant depolarization after treatment with PP2 (absolute membrane potential (-22.5±2.4mV; n=39) or transfection with siC-Src (-14.2±2.4mV; n=14) or with siFyn (-14.5±3mV; n=14) compared to control (-40±3.2mV; n=36) or to cells treated with PP3 (-43±1.3mV; n=4) or transfected with nsRNA (-38±4.5mV; n=18) (Figure 9). Taken together, these data further strengthen the role of TASK-1 and the importance of SrcTK in setting the negative resting membrane potential in primary PASMCs.

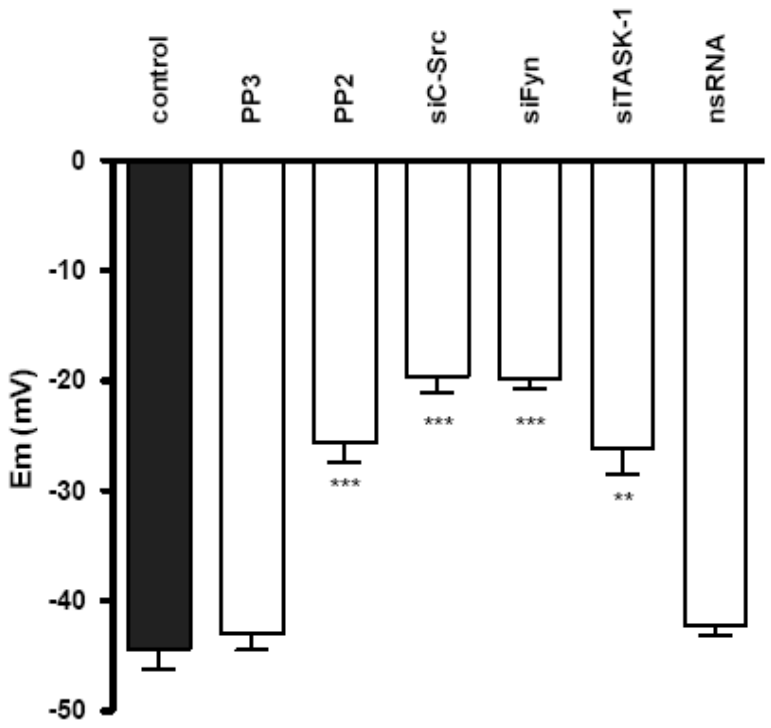

Figure 9. Role of SrcTk for the resting membrane potential of primary hPASMC.

The histograms summarizes the effects of SrcTK inhibition on the resting membrane potential of hPASMCs. Significant depolarization was observed when the cells were treated

with PP2 (1 μM) or transfected with siC-Src, siFyn or siTASK-1, but not after transfection with nsRNA and treatment with PP3.

Hypoxic regulation of SrcTK in hPASMCs

The SH1 domain of SrcTK contains the phosphorylation site tyr419 which is required for full C-SrcTK activation. This mechanism allows C-SrcTK to interact with ion channels and modulate their properties(Alioua *et al.*, 2002). Inactivation of human C-SrcTK occurs when its C-terminal tyr530 is phosphorylated which then binds to the SH2 domain. Crystallographic studies have shown that interactions between the C-terminus and the SH2 domain, and between the kinase domain and the SH3 domain, cause the C-SRC molecule to assume a closed configuration that covers the kinase domain and reduces its potential for substrate interaction(Dai *et al.*, 2009).

Since the activity of SrcTK is determined by the phosphorylation state of SrcTK at tyr419, we next investigated the phosphorylated (active, Figure 3.10A upper panel) and non-phosphorylated (inactive, Figure 3.10A middle panel) state of SrcTK in hPASMCs in normoxia and at different time points under hypoxia (-30 or normoxia, 0, 1, 5, 10, 15, 20 and 30 minutes of hypoxia). The lower panel of Figure. 7B clearly shows the reduced phospho-SrcTK staining in hypoxia.

Hypoxia, as well as application of the SrcTK-inhibitor PP2, decreased the tyrosine-phosphorylation state of TASK-1 channels, whereas PP3, the inactive analog of PP2, did not change the TASK-1-phosphorylation (Figure 3.10B). the lower panel shows the unchanged total level of TASK-1 under different experimental conditions.

Then, the co-localization of the background TASK-1 channel (green) and phospho-SrcTK (red) was examined in hPASMC under normoxia and in 15 minutes hypoxia and visualized by confocal laser scanning microscopy (Figure 3.10C).

A

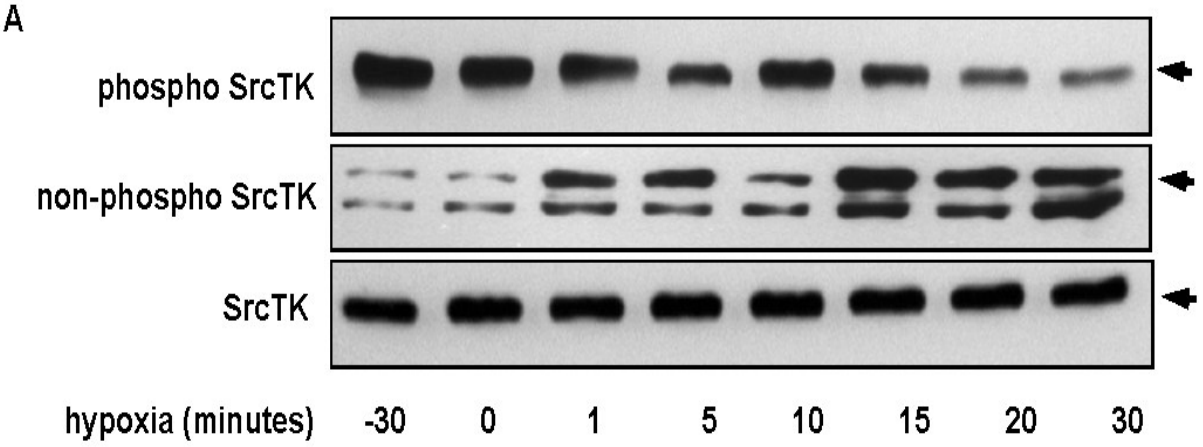
phospho SrcTK
non-phospho SrcTK
SrcTK
hypoxia (minutes)
-30
0
1
5
10
15
20
30

B

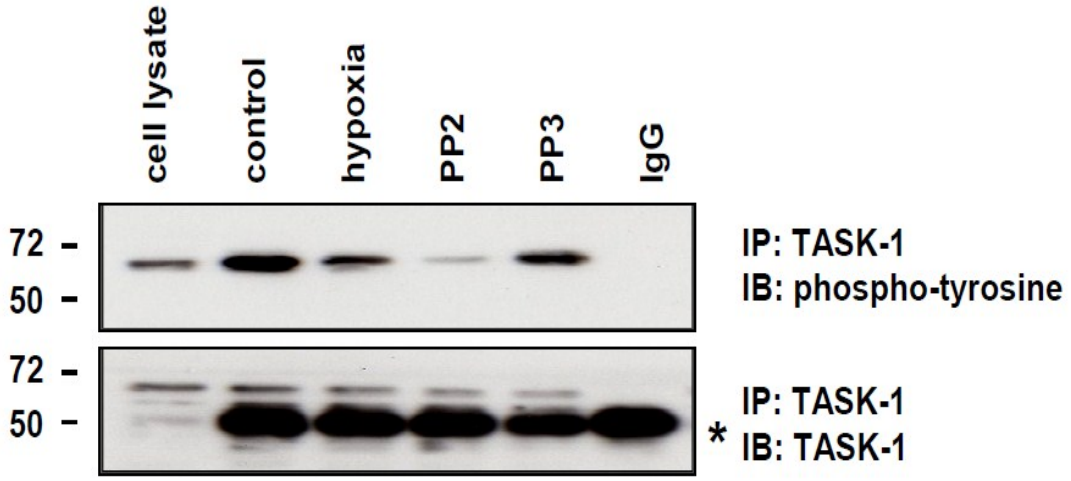
cell lysate
control
hypoxia
PP2
PP3
IgG
72
50
IP: TASK-1
IB: phospho-tyrosine
72
50
IP: TASK-1
IB: TASK-1
*

C

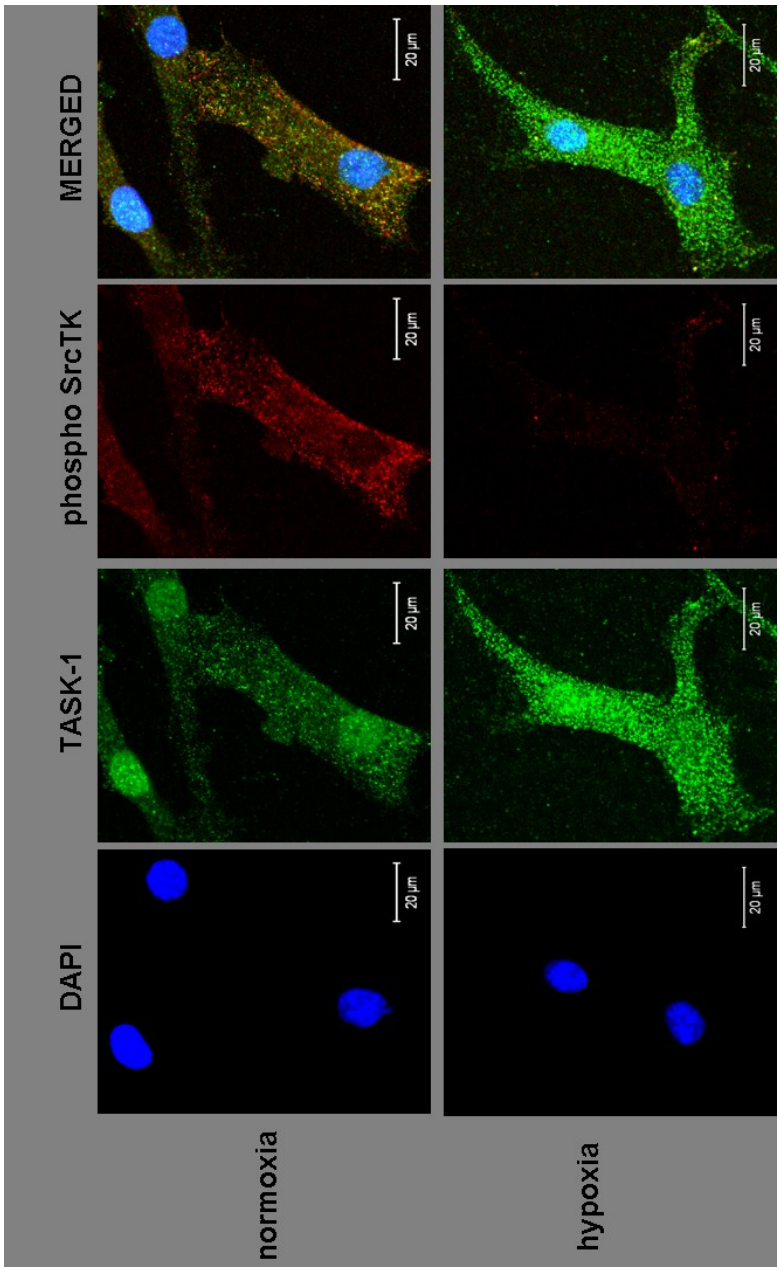

Figure 3.10. Effect of hypoxia on SrcTK phosphorylation in primary hPASMCs.

(A) Hypoxia decreased phospho-SrcTK (tyr-419) immunoreactivity (60 kDa), whereas enhanced immunoreactivity was detected at the non-phospho SrcTK (60-65 kDa) in a time-dependent manner. Protein loading equivalence is shown by total SrcTK (n=4). **(B)** Application of hypoxia or the SrcTK-inhibitor PP2 decreased the tyrosine-phosphorylation state of TASK-1 channel. **(C)** An evident decrease of phospho-SrcTK is shown in immuno

co-localization of TASK-1 (green) and phospho-SrcTK tyr-419 (red) after 15 minutes of hypoxia compared to normoxia.

SrcTK activator affects TASK-1 current in primary hPASMC

Next, the functional role of SrcTK for the hypoxic inhibition of the TASK-1 channels was examined. Intracellular application of SrcTK activator peptide significantly increased TASK-1 current density. Dialysis with Src activator peptides (EPQYEEIPIYL) also significantly increased the TASK-1 current density (0.72±0.05 pA/pF; n=8) compared to control (0.51±0.05 pA/pF; n=10) (Figure 3.11). Figure 3.12A summarizes the effects of SrcTK activator peptides. As the initial TASK-1 current was decreased by inhibiting SrcTK with blocker or siRNA, hypoxia did not have any further effect on cells treated with PP2 or transfected with siC-Src or siFyn. However, hypoxia still was able to inhibit the TASK-1 current in control, PP3-treated or nsRNA transfected hPASMCs. Relative TASK-1 currents under hypoxia in hPASMCs are presented in Figure 3.12B.

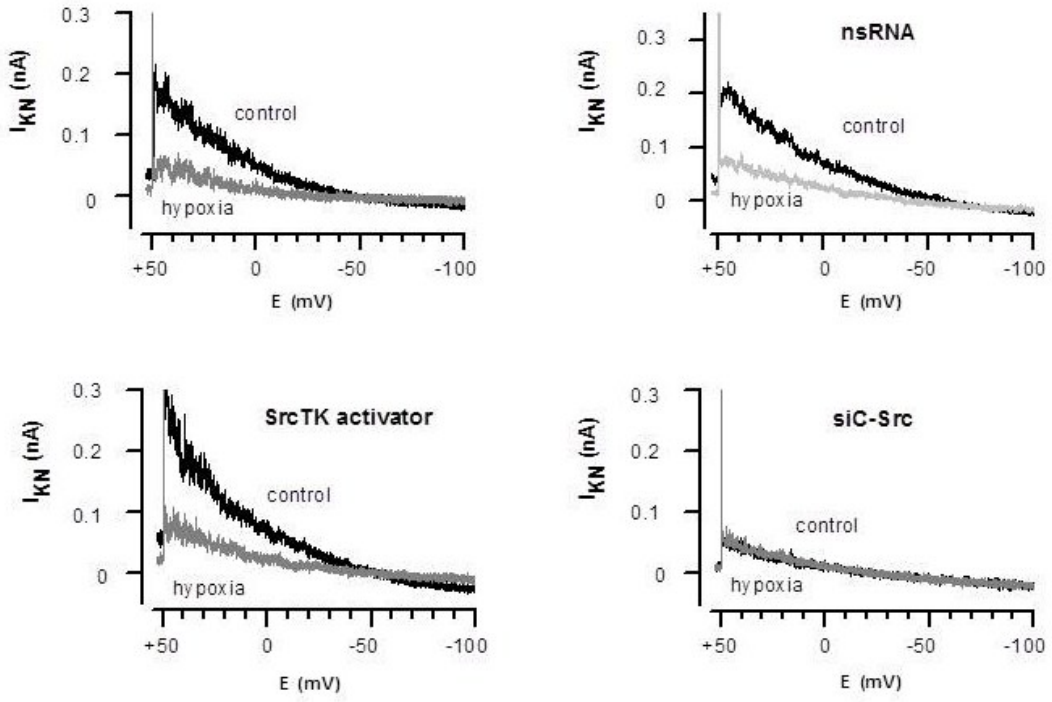

Figure 3.11. SrcTK activator on TASK-1. Representative recordings of TASK-1 current (I_{KN}) control and under hypoxia without (upper panel) or with (lower panel) SrcTK activator peptide, EPQYEEIPIYL (1 mM) in the patch pipette.

A **B**

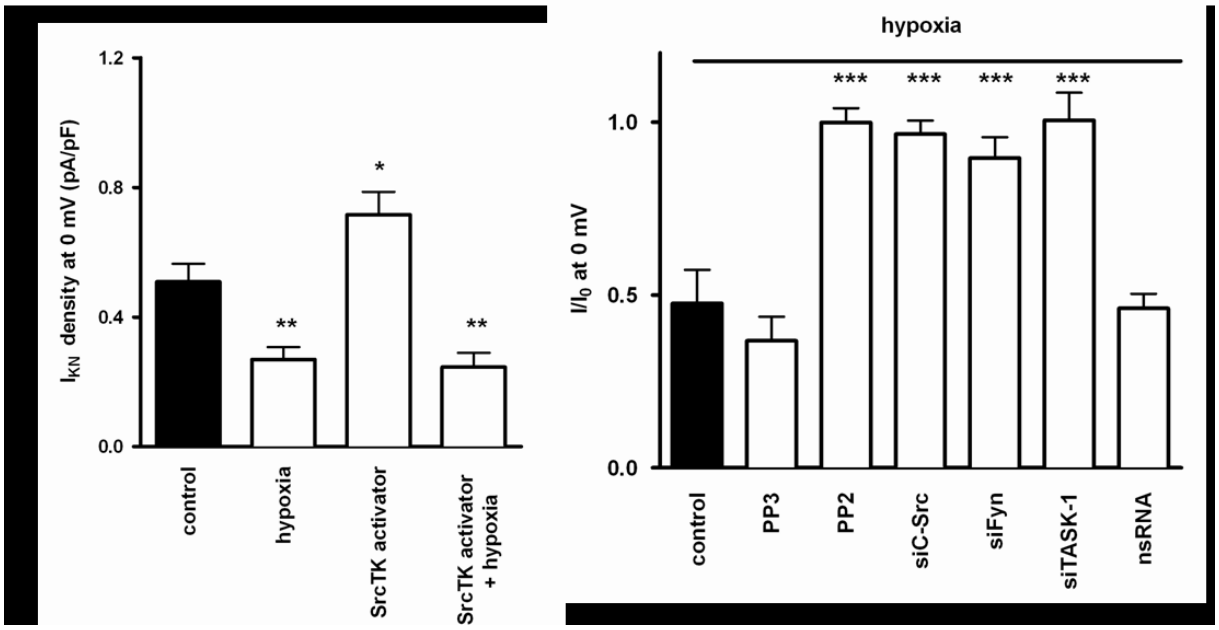

Figure 3.12. Effects of the intracellularly applied SrcTK activator on TASK-1 current density and relative current.

(A) Bar graph summaries the significant increase of the current density of TASK-1 current compared to the control after application of the SrcTK activator peptide. This increased TASK-1 current is significantly inhibited by hypoxia. **(B)** Histogram summarizing the lack of hypoxia-induced TASK-1 current inhibition after treatment with PP2, siC-Src, siFyn, and siTASK-1.

Impact of SrcTK on the hypoxia-induced increase of intracellular calcium ($[Ca^{2+}]_i$) in hPASMCs

Hypoxia-induced $[Ca^{2+}]_i$ rise is an integral and characteristic property of hPASMCs, which is directly linked to downstream signaling which results in vasoconstriction. Therefore, we further analyzed the role of SrcTK in the hypoxia-induced $[Ca^{2+}]_i$ rise in hPASMCs. Fluo4-loaded hPASMCs were continuously monitored for changes in $[Ca^{2+}]_i$ under hypoxia (Figure 3.13A). Hypoxia significantly increased $[Ca^{2+}]_i$ in control cells (0.5365±0.04), in cells treated with PP3 (0.5161±0.04) or transfected with nsRNA (0.4540±0.06). In contrast, the hypoxia-induced increase in $[Ca^{2+}]_i$ was markedly attenuated after treatment with PP2 (0.185±0.01), transfection with siC-Src (0.1228±0.01) siFyn (0.1199±0.01), or siTASK-1 (0.2524±0.01). Summarized results are presented in Figure 3.13B.

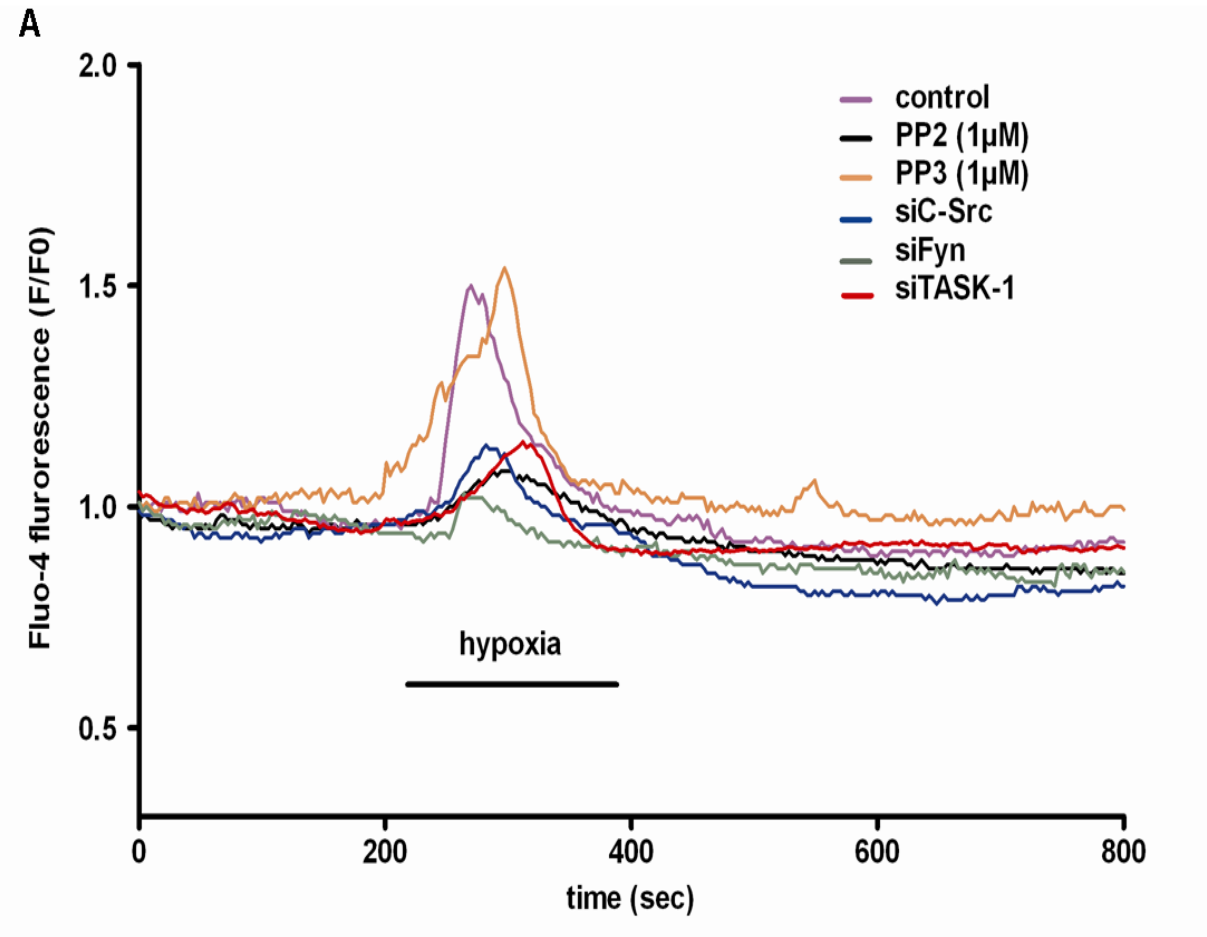

B

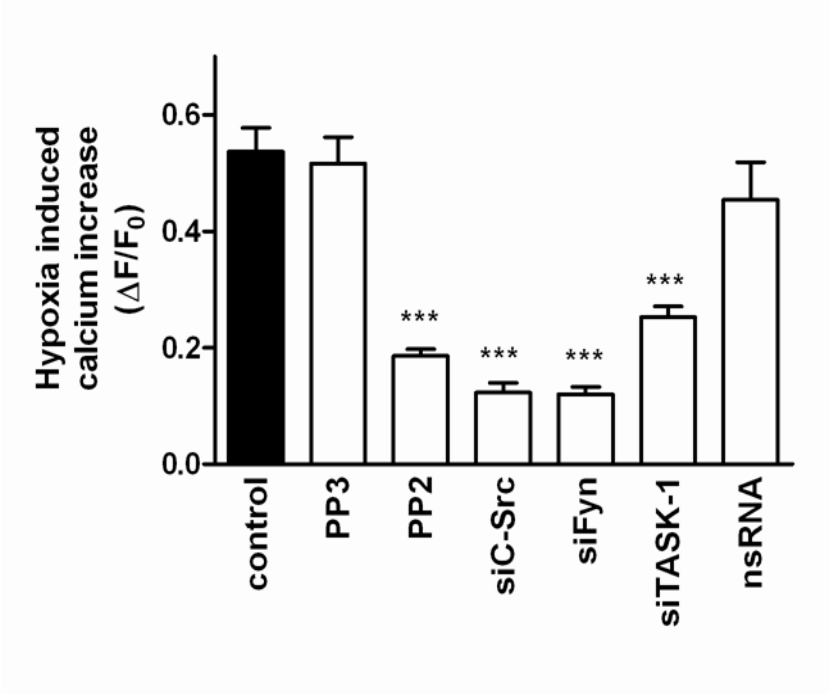

Figure 3.13. Inhibition of SrcTK attenuates hypoxia-induced increase in intracellular $[Ca^{2+}]_i$ in primary hPASMCs.

(A) Representative recordings of fluo-4 fluorescence after hypoxic challenge in a control hPASMC and in cells treated with PP2, PP3, siC-Src, or siFyn. **(B)** Hypoxia-induced increase in intracellular $[Ca^{2+}]_i$ was decreased after treatment with PP2, siC-Src or siFyn, but not with nsRNA or PP3. (supported by Zoltan Balint, MD PhD)

Inhibition of SrcTK attenuates Kv current in hPASMCs

Impact of SrcTK inhibition on whole-cell potassium currents, voltage-gated (Kv) channels and calcium-activated potassium (KCa) was investigated in primary human PASMCs. Representative Kv current recordings in control hPASMCs and after treatment with siC-Src are presented in Figure 3.14 showing that silencing of C-Src and Fyn significantly decreases the Kv current.

To further assess the role of SrcTK for the activation of Kv and KCa channels, the effect of PP2, PP3 and the treatment with siC-Src, siFyn or nsRNA was investigated and compared with the effect of hypoxia (Figure 3.14C). Treatment of hPASMCs with PP2 (3.76±0.3 pA/pF; n=16), or siC-Src (2.95±0.3 pA/pF; n=5) or siFyn (3.06±0.2 pA/pF; n=5) significantly decreased the Kv current compared to control (8.95±0.7 pA/pF; n=24,). Hypoxia showed a similar effect (Figure 3.14C). Treatment with PP3 (9.33±0.7 pA/pF; n=4) or transfection with nsRNA (7.82±0.4 pA/pF; n=9) did not alter the current (Figure 3.14C).

A

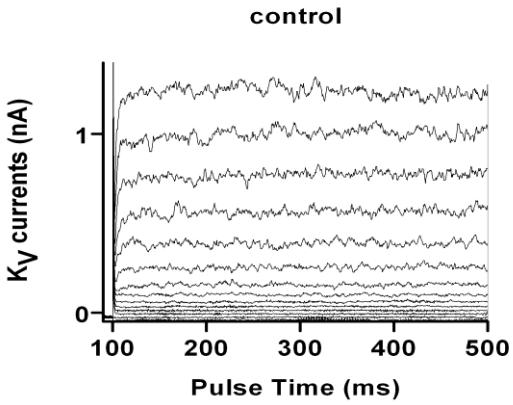

B

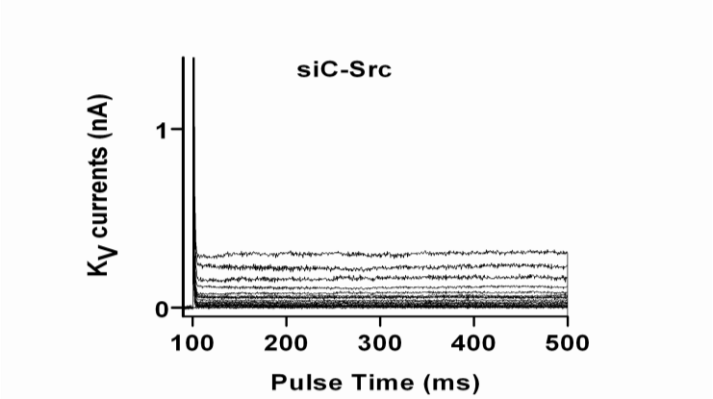

C

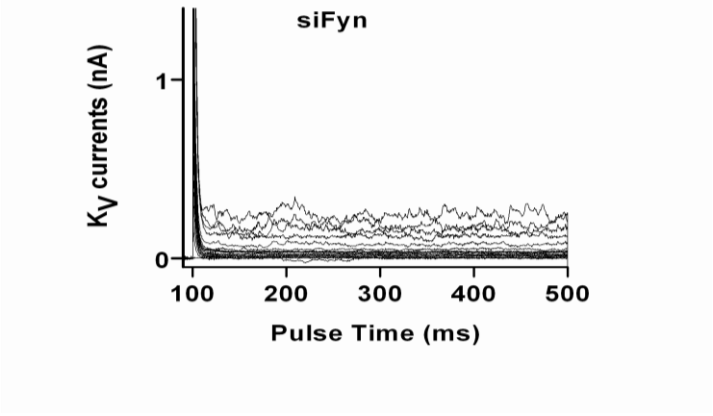

D

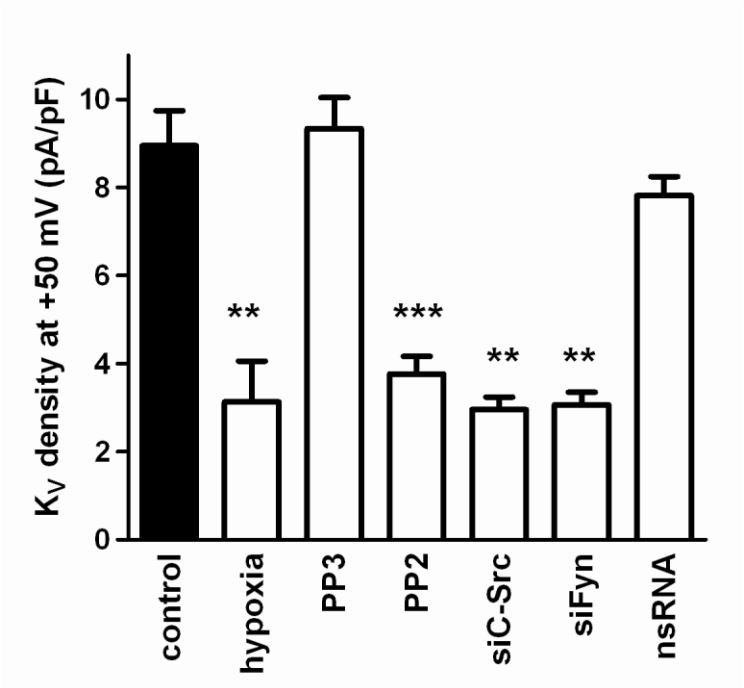

Figure 3.14. Effect of silencing of C-Src or C-Fyn on voltage-gated (Kv) current in primary hPASMC (A) Representative recordings of Kv in normoxia. **(B)** Reduced Kv current in normoxia after treatment with siC-Src or siFyn **(C)**. **(D)** Histograms summarizing

the effects of hypoxia, PP3, PP2, siC-Src, siFyn or nsRNA for Kv current density (supported by Bi Tang, MD PhD)

Inhibition of SrcTK attenuates KCa current in hPASMCs

The Impact of SrcTK inhibition on calcium-dependent potassium current (KCa), was also investigated in primary human PASMCs. Representative KCa current recordings in control hPASMCs are shown in Figure 3.15A. Figure 3.15B and 3.15C show that after silencing of siC-src and siFyn the KCa current is significantly decreased.

To further assess the role of SrcTK for activation of KCa channels, the effect of PP2, PP3 and the effect of silencing of siC-Src, siFyn or nsRNA was investigated and compared with the effect of hypoxia (Figure 3.15D). Only hypoxia (2.3±0.5 pA/pF; n=16), treatment with PP2 (4±0.3 pA/pF; n=17), siC-Src (2.35±0.6 pA/pF; n=5) or siFyn (1,81±0.4 pA/pF; n=5) decreased the current compared to control (5.7±0.6 pA/pF; n=12), whereas PP3 (5.58±0.3 pA/pF; n=5) or nsRNA (5.17±0.9 pA/pF; n=8) had no significant effects (Figure 3.15D).

A

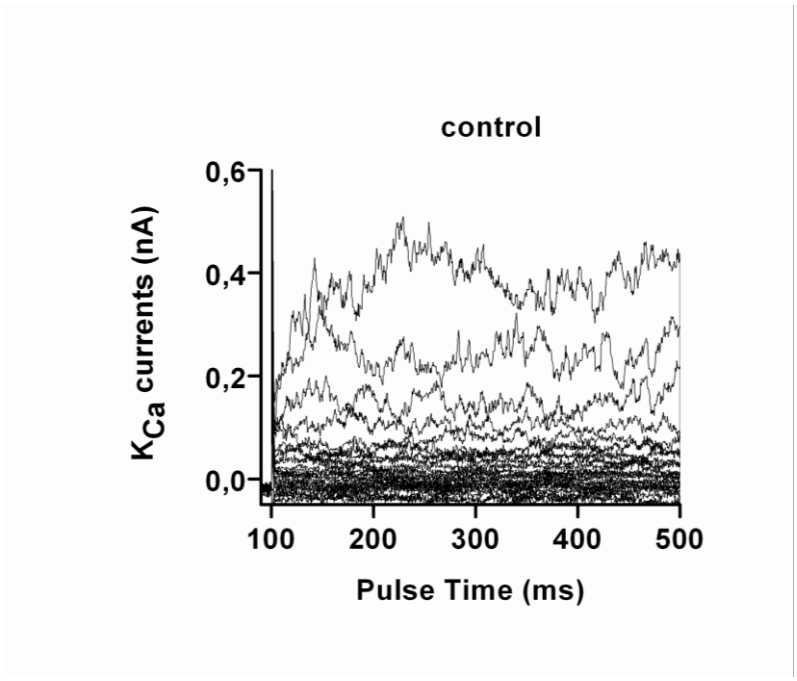

B

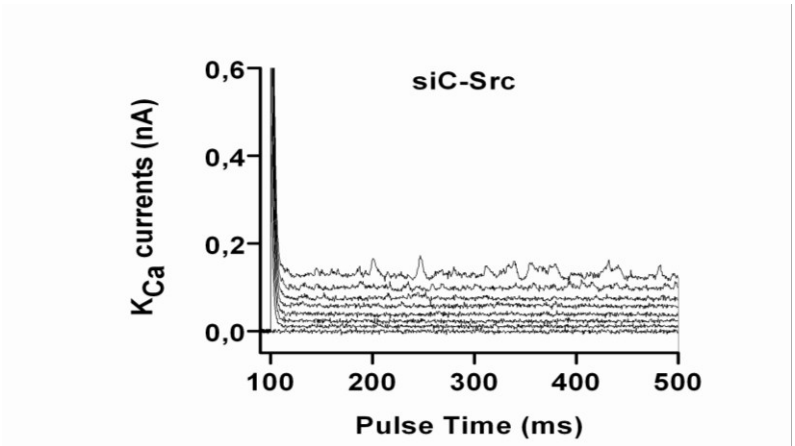
siC-Src
K_{Ca} currents (nA)
0,6
0,4
0,2
0,0
100
200
300
400
500
Pulse Time (ms)

C

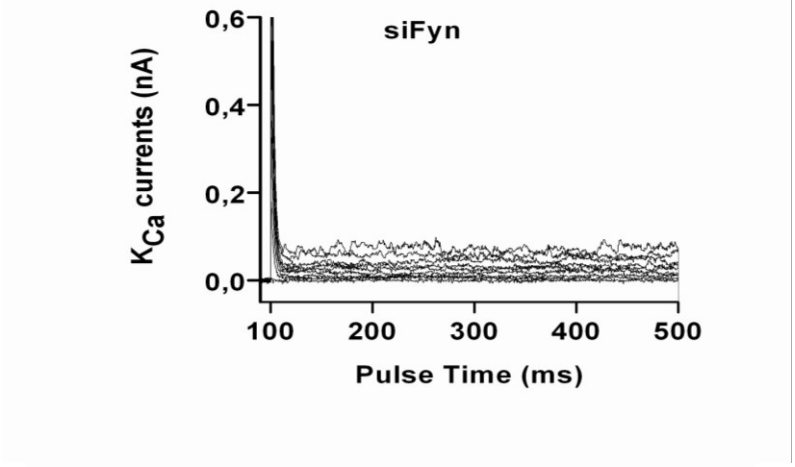
siFyn
K_{Ca} currents (nA)
0,6
0,4
0,2
0,0
100
200
300
400
500
Pulse Time (ms)

D

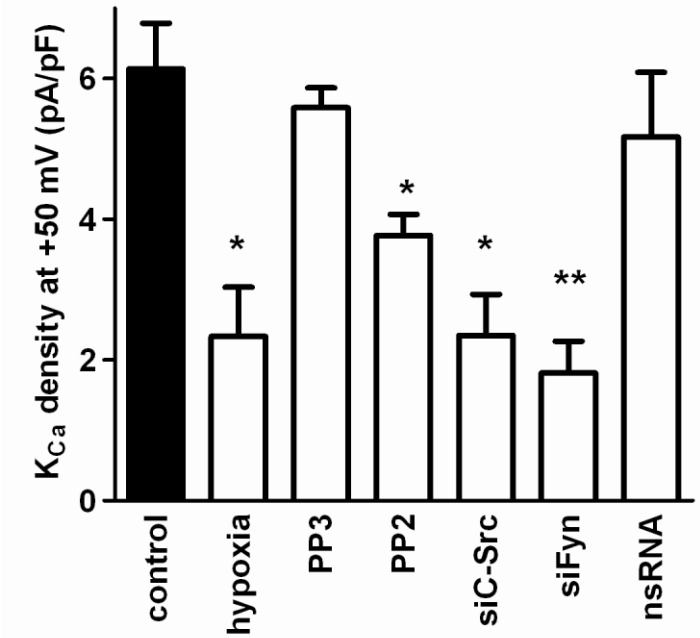
K_{Ca} density at +50 mV (pA/pF)
0
2
4
6
*
*
*
**
control
hypoxia
PP3
PP2
siC-Src
siFyn
nsRNA

Figure 3.15. Effect of silencing of C-Src or C-Fyn on the calcium activated potassium current (KCa) in primary hPASMC (A) Representative recordings of KCa in normoxia. Reduced KCa current in normoxia after treatment with siC-Src **(B)** or with siFyn **(C)**. **(D)** Histograms summarizing the effects of hypoxia, PP3, PP2, siC-Src, siFyn or nsRNA for the KCa current density (supported by Bi Tang, MD PhD)

Pulmonary vasoconstriction in response to SrcTK inhibitors

To depict the role of SrcTK in the pulmonary vascular tone, we used the isolated perfused mouse lung model. Our investigations showed that PP2 (6.3±1.31 mmHg: n=4) caused a significant increase in pulmonary arterial pressure compared to the vehicle control (dmso) or to the effect of the inactive analog PP3 (0.6±0.2 mmHg: n=4). Furthermore, dasatinib, the clinically-used drug for the treatment of Chronic myelogenous leukemia (CML) which is a potent inhibitor for SrcTK, showed a similar increase (5.5±0.2 mmHg: n=3) in pulmonary pressure compared to the solvent control (dmso; 0.4±0.4 mmHg: n=4). Figure 3.16 shows the summarized changes in the pulmonary arterial pressure under PP2, PP3, dmso, and dasatinib treatment.

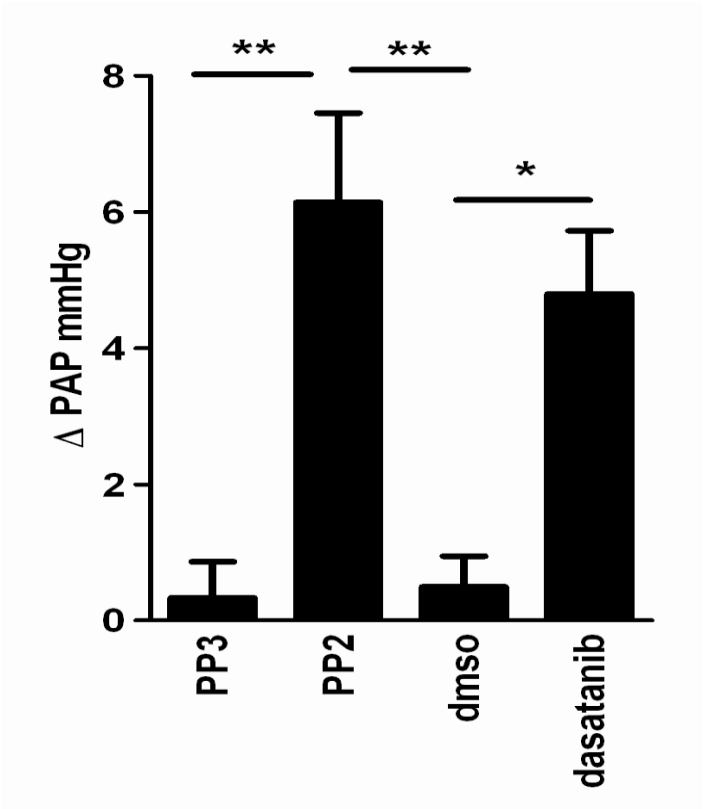

Figure 3.16. Effect of the SrcTK inhibitor dasatinib on the pulmonary artrial pressure. The histogram summarizes the changes in pulmonary artery pressure in the presence of PP2, PP3 and dasatinib, expressed as delta PAP mmHg from baseline in isolated perfused mouse lungs.

Discussion

Discussion

Modulation of TASK-1 channels by G protein-coupled pathways, with special focus on protein kinase C

TASK-1 sets the resting membrane potential in primary human pulmonary artery smooth muscle cells and hPASMCs, as our group has previously shown by means of TASK-1–siRNA studies (Olschewski et al, Circ res 2006). Several studies have examined the mechanisms by which a G protein–coupled receptor agonist may inhibit two-pore domain K^+ channels. These studies showed that G protein–coupled receptor agonist-induced inhibition of the two-pore domain K^+ channels was due to distinct pathways in different cell types ATP-dependent pathways (Enyeart *et al.*, 2005),depletion of PIP_2 levels(Lopes *et al.*, 2005), direct action of DAG and phosphatidic acid that are generated via PLC (Chemin *et al.*, 2003)or elevated intracellular Ca^{2+} levels (Enyeart *et al.*, 2005)activated the Gαq pathway in different systems. Moreover, a very recent study proposes a direct interaction of Gαq with TASK-1 in a mammalian heterologous expression system(Chen *et al.*, 2006).

The role of TASK-1 for endothelin-induced pulmonary vascoconstriction

We investigated the effect of one of the most potent vasoconstrictors Endothelin-1 (ET-1) in the pulmonary circulation, since the activated endothelin system significantly contributes to the pathologic changes in pulmonary hypertension(Stewart *et al.*, 1991), and ET receptor antagonists have been shown to be effective for the therapy of pulmonary artrial hypertension (PAH) (Miyauchi *et al.*, 1993). Circulating ET-1 levels are elevated in animal models of PAH (Rubin *et al.*, 2002)as well as in human PAH (Stewart *et al.*, 1991)In addition, a correlation between increased ET-1 expression in the lung of patients with pulmonary hypertension and the severity of the disease has been demonstrated(Giaid *et al.*, 1993). Although, this evidence indicates that the ET system plays a key role in the pathogenesis of pulmonary hypertension, the molecular targets of ET-1 have not been characterized in detail.

We found that PLC inhibition abolished the ET-1 effect on TASK-1 indicating that PLC is required, which is in in *Xenopus laevis* oocytes (Czirjak *et al.*, 2001) in contrast to the report in a mammalian heterologous expression system() .Additional evidence comes from the use of COS-7 cells expressing TWIK-related K^+(TREK)-2 and muscarinic receptor M_3, in which the same PLC inhibitor was applied to prevent acetylcholine-induced inhibition of TREK-2 (Kang *et al.*, 2006). The inhibitory effect of the PIP_2 scavenger on TASK-1 observed in this study confirms previously reported results obtained with different two-pore domain K^+ channels expressed in *Xenopus* oocytes(Lopes *et al.*, 2005) ,and strongly suggests that PIP_2 hydrolysis by PLC indeed affects channel activity. Moreover, we showed that the downstream product of PIP_2 hydrolysis DAG, underlies the agonist-induced inhibition of TASK-1 in hPASMCs. These results are further supported by our experiments showing that the DAG kinase inhibitor abolished the ET-1 effect on TASK-1.

In conclusion, our results suggest that the TASK-1 modulation by the Gαq pathway in primary hPASMCs achieved by signaling rather than direct interaction between PIP_2 and TASK-1 in primary hPASMCs figure 4.1(Lopes *et al.*, 2005)

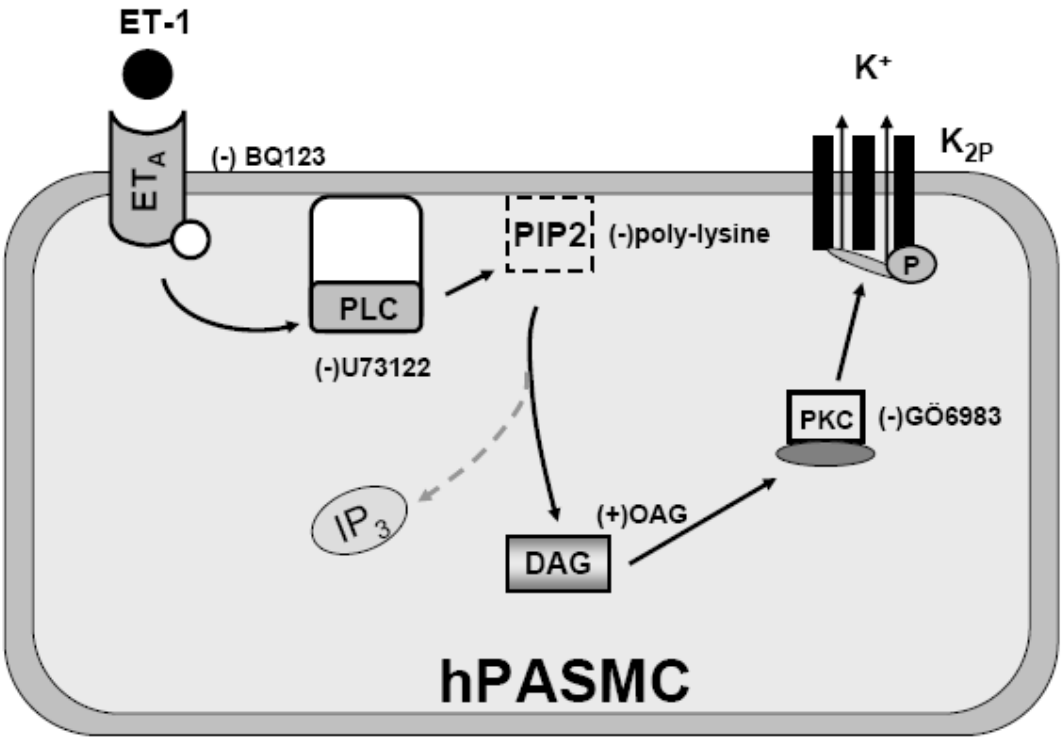

Figure 4.1. Schematic presentation of the ET-1 signaling pathway in hPASMCs

ET-1 binds to the G protein-coupled-receptor (Gαq) ETA, leading to the protein kinase C (PKC)-induced phosphorylation of TASK-1 channels through phospholipase C (PLC), phosphatidylinositol 4,5-biphosphate (PIP2) and diacylglycerol (DAG). (+) indicate agonist and (-) indicate antagonist effects.(Tang *et al.*, 2009)

Modulation of TASK-1 channel by hypoxia

The main findings of this study are that 1) two members of the SrcTK family, C-Src and Fyn, are highly expressed in primary human pulmonary artery smooth muscle cells 2) TASK-1 channels and SrcTK are co-localized in the plasma membrane of hPASMCs; 3) SrcTK is required for the activity of TASK-1 channels; 4) the inhibition of SrcTK depolarizes hPASMCs; 5) hypoxia reduces the tyrosin phosphorylation level of TASK-1; 6) hypoxia reduces the active phosphorylated state of SrcTK and inhibits TASK-1 current facilitated by a SrcTK activator; 7) SrcTK inhibition markedly attenuates the hypoxia-induced intracellular calcium rise; 8) the whole cell potassium current (K_v and K_{Ca}) is reduced by SrcTK inhibition and 9) inhibition of SrcTK by PP2 or dasatinib causes a substantial increase in the pulmonary arterial pressure of isolated perfused mouse lungs.

The role of potassium channels for the vascular tone in pulmonary arteries

The membrane potential of smooth muscle cells is an important factor in controlling the pulmonary vascular tone. At rest, the membrane potential of PASMCs is approximately –50mV{Gurney, 2003 1360 /id}-{Gurney, 2002 1430 /id}{Olschewski, 2006 1734 /id}. This is maintained by K^+ efflux from these cells through K^+ channels. Agents that inhibit or activate pulmonary vascular smooth muscle cell K^+ channels cause depolarization or hyperpolarization, respectively. The function, control and expression of K^+ channels in pulmonary arteries is a matter of continued interest, because it is likely that a decrease in K^+ channel expression(Platoshyn *et al.*, 2001, Yuan *et al.*, 1998) or a dysfunction of K^+ channels gives rise to membrane depolarization{Yuan, 1998 1033 /id} and, together with an increase in the cytosolic calcium, results in increased proliferation and decreased apoptosis, ultimately contributing to the pathogenesis of pulmonary hypertension(Mandegar *et al.*, 2004).

Depolarization in hPASMCs, induced by the inhibition of K^+ channels, is followed by an influx of calcium through the voltage-gated (L-type) calcium channels and finally results in increased pulmonary vascular resistance. Acute hypoxia causes vasoconstriction by several mechanisms. It depolarizes PASMCs by inhibiting K^+ channels, leading to calcium influx as described above(Post *et al.*, 1992), it causes the release of calcium from the sarcoplasmic reticulum (SR) and subsequent repletion through store-operated channels(Vadula *et al.*, 1993),acute hypoxia induced increases calcium influx into PASMCs through the L-type Ca

channels, independent of the membrane potential (del Valle-Rodriguez *et al.*, 2003)and also promotes calcium sensitization, thus increasing pulmonary vascular resistance.(Robertson *et al.*, 2003) Most of the calcium responsible for the increase in cytosolic calcium induced by hypoxia comes from outside the PASMC but some is released from internal stores such as the SR(Weir *et al.*, 2010, Weir and Olschewski, 2006). It is likely that the reduction in the hypoxia-induced increase in calcium that is caused by PP2, or siC-Src, or siFyn (results Figure 3.13), is secondary to the lack of hypoxic inhibition of K^+ currents, because inhibition of K^+ channels has already been caused by SrcTK inhibition. The hypoxic response is abolished in the presence of diminished SrcTK activity (results Figure 3.12).

Modulation of potassium channels by tyrosine kinases

Several studies have indicated that tyrosine kinases may act on K^+ channels. However, these studies were carried out on cell lines or in heterologous expression systems using a broad range of inhibitors but without showing the physiological role of the findings(Holmes *et al.*, 1996, Holmes *et al.*, 1997). Our group has previously shown that the background two pore domain TASK-1 channel sets the membrane potential in primary human PASMCs, and it can be modulated by PKA, PLC, PKC and AMPK pathways through serine-threonine phosphorylation by different agonists, such as endothelin(Tang *et al.*, 2009) treprostinil(Li *et al.*, 2012) etc. Furthermore, hypoxia depolarizes the membrane potential by reversibly inhibiting the TASK-1 channels in hPASMC(Olschewski *et al.*, 2006). In addition, K_{Ca} and K_v channels may also contribute to the membrane potential, particularly if they are stimulated by agents like cAMP and cGMP. Therefore, our results suggest that the SrcTK activity is essential for the low physiologic tone of PASMC and thus, for the low pulmonary vascular resistance.

The mechanism by which hypoxia inhibits these channels is currently unknown. However, in our investigations, specific inhibition of endogenous SrcTK reduces TASK-1 current in hPASMC. Likewise, when hPASMCs are dialysed with SrcTK activator, a significant increase in the TASK-1 current is observed, suggesting that the TASK-1 current requires SrcTK activity with dephosphorylation decreasing the current and phosphorylation increasing it. Several other potassium channels, including K_v and K_{Ca}, have previously been shown to be modulated by SrcTK-mediated tyrosine phosphorylation(Alioua *et al.*, 2002). Our observations confirm this findings but demonstrate the critical role of ScrTK activity for

the function of these channels and furthermore show that TASK-1 activity requires SrcTK activity.

In the present study, we demonstrated that SrcTK inhibition reduces the TASK-1 current and plays a crucial role in the hypoxic inhibition of TASK-1 channels, probably through a reduction in phosphorylation of SrcTK at tyr419 and dissociation of TASK-1 and SrcTK, although the molecular regulation of this link has yet to be determined (Figure 4.2).

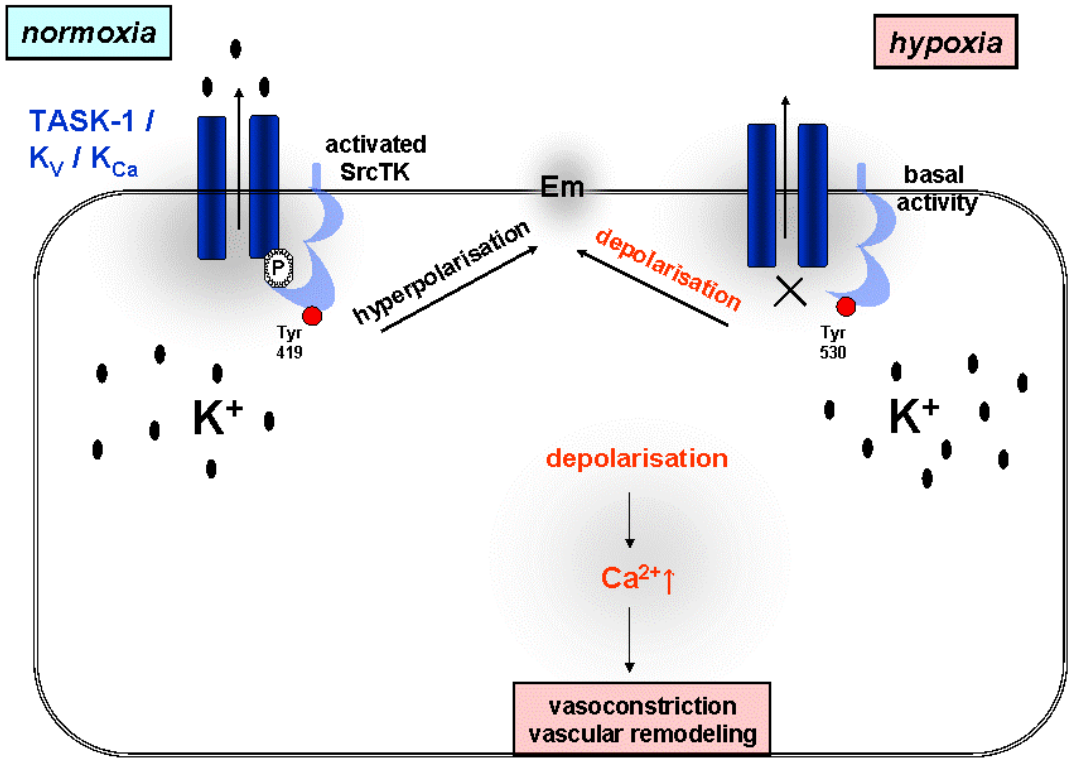

Figure 4.2 . Scheme of the proposed interplay between TASK-1 channel and c-Src in human PASMCs.

Under normoxia, the phospho-Src (active-Src, phosphorylated at Tyr419) binds to TASK-1 channels resulting in functional TASK-1 channels. Active TASK-1 channels maintain negative resting potential in hPASMCs. In hypoxia, the phospho-Src (active-Src) is decreased. Closed TASK-1 leads to depolarisation and increased intracellular calcium level. (+) indicate increase and (-) indicate decrease. Em: resting membrane potential, TASK-1: TWIK-related acid sensitive potassium channel-1.

A recent study by Knock et al. describes that SrcTK inhibition by PP2 blunts hypoxia-induced pulmonary vasoconstriction and inhibits Rho kinase in rat pulmonary artery and isolated PASMC(Knock *et al.*, 2008b, Knock *et al.*, 2008a). Their finding that PP2 reduces the hypoxia-induced increase in PASMC cytosolic calcium is concordant with our observations. Given the inhibitory results of PP2 and the siRNAs on TASK-1, K_v and K_{Ca} currents that we describe here, and the similar effects of hypoxia on these currents, it makes sense that the SrcTK phosphorylation is inhibited in the sequence leading to the K^+ current inhibition. However, in their experiments hypoxia increased phosphorylation of SrcTK at tyr419 rather than decreased it, compare to our study. The difference in these results may be due to differences in species, cell culture conditions, the number of cycles, and the severity, duration or time point of the study under hypoxia.

Tyrosine kinase increases pulmonary vascular tone

The observed increase in PAP followed by the inhibition of SrcTK by PP2 and dasatinib suggests a functional role for SrcTK in regulating pulmonary vascular tone. It is an open question what this means for patients with severe pulmonary hypertension. Tuder et al. describe decreased levels of c-Src in sixteen PPH (IPAH according to the current classification) patients(Tuder *et al.*, 2001). This corresponds to a decreased potassium channel activity and might contribute to vasoconstriction and other pathologic mechanisms leading to pulmonary hypertension. Here we report a reduced TASK-1, whole-cell K current and K_{Ca} current after c-Src inhibition in hPASMC. This is in line with observations showing that reduced Kv1.5 activity leads to pulmonary hypertension. In contrast, a recent study by Courboulin et al. reports increased levels of phosphor-Src and total Src in lung samples from three PAH patients(Courboulin *et al.*, 2011).

Recent clinical observations highlight the potential importance of tyrosine kinases in the pathophysiology of PAH. Chronic myeloid leukemia (CML) is caused by a constitutively active BCR-ABL tyrosine kinase. Imatinib, which inhibits this kinase, is the first–line therapy for CML(Kantarjian *et al.*, 2010). Imatinib is also an effective inhibitor of the platelet-derived growth factor receptor(Schermuly *et al.*, 2005) and this is thought to be the reason why it may improve hemodynamics in some PAH patients(Ghofrani *et al.*, 2010a, Ghofrani *et al.*, 2010b). Dasatinib is a tyrosine and a serine/threonine kinase inhibitor, which is 325 times as potent as imatinib in the inhibition of BCR-ABL kinase in vitro and induces higher and faster rates of

cytogenic response in CML(Mattei *et al.*, 2009). However, dasatinib potently inhibits the Src family, which is probably the single most prominent dasatinib-targeted family of protein kinases including C-Src and Fyn and it has been reported to cause pulmonary arterial hypertension(Dumitrescu *et al.*, 2011, Kantarjian *et al.*, 2010, Mattei *et al.*, 2009). The pulmonary hypertension tends to resolve rapidly after discontinuation of dasatinib(Dumitrescu *et al.*, 2011), suggesting that it may not be primarily due to marked cellular proliferation, but to chronic vasoconstriction. we conclude that dasatinib-initiated pulmonary hypertension relate to our finding that siRNA against C-Src and Fyn reduces potassium channel current and causes depolarization of hPASMCs. It is clear that much work remains to be done in order to clarify the role of different kinases in the etiology and therapy of PAH.

Limitations of the study

Although the present findings suggest that TASK-1 channels and SrcTK are co-localized in the plasma membrane of hPASMCs, which is further supported by co-immunoprecipitation studies, we cannot exclude that SrcTK could also act indirectly on potassium channels via other Src downstream molecules. In addition, mechanism(s) involved in acute hypoxia-induced inhibition of potassium channels could be different than those involved in chronic exposure to hypoxia and/or dasatinib. Finally, changes in the pulmonary artery pressure in the presence of PP2 and/or dasatinib might not be related to this precise proposed mechanism.

Conclusion

In conclusion, we demonstrate that SrcTK plays an important role in the modulation of TASK-1 and other potassium channels and that it sets the negative resting membrane potential in hPASMCs. The physiological relevance of this SrcTK and TASK-1 channel association is emphasized by the fact that hypoxia-induced inhibition of the TASK-1 current and the intracellular calcium rise is dependent on SrcTK. It is very likely that a better description of the multifunctional role of SrcTK in regard to K^+ channel regulation facilitates our understanding of the pathophysiology of pulmonary hypertension.

References

References

Alioua, A, Mahajan, A, Nishimaru, K, Zarei, MM, Stefani, E & Toro, L (2002). Coupling of c-Src to large conductance voltage- and Ca2+-activated K+ channels as a new mechanism of agonist-induced vasoconstriction. *Proc Natl Acad Sci U S A* **99**: 14560-5, 10.1073/pnas.222348099.

Archer, SL, Souil, E, Dinh-Xuan, AT, Schremmer, B, Mercier, JC, El Yaagoubi, A*, et al.* (1998). Molecular identification of the role of voltage-gated K+ channels, Kv1.5 and Kv2.1, in hypoxic pulmonary vasoconstriction and control of resting membrane potential in rat pulmonary artery myocytes. *J Clin Invest* **101**: 2319-30, 10.1172/JCI333.

Chemin, J, Girard, C, Duprat, F, Lesage, F, Romey, G & Lazdunski, M (2003). Mechanisms underlying excitatory effects of group I metabotropic glutamate receptors via inhibition of 2P domain K+ channels. *EMBO J* **22**: 5403-11, 10.1093/emboj/cdg528.

Chen, X, Talley, EM, Patel, N, Gomis, A, McIntire, WE, Dong, B*, et al.* (2006). Inhibition of a background potassium channel by Gq protein alpha-subunits. *Proc Natl Acad Sci U S A* **103**: 3422-7, 10.1073/pnas.0507710103.

Choe, S (2002). Potassium channel structures. *Nat Rev Neurosci* **3**: 115-21, 10.1038/nrn727.

Courboulin, A, Paulin, R, Giguere, NJ, Saksouk, N, Perreault, T, Meloche, J*, et al.* (2011). Role for miR-204 in human pulmonary arterial hypertension. *J Exp Med* **208**: 535-48, 10.1084/jem.20101812.

Czirjak, G, Petheo, GL, Spat, A & Enyedi, P (2001). Inhibition of TASK-1 potassium channel by phospholipase C. *Am J Physiol Cell Physiol* **281**: C700-8.

Dai, S, Hall, DD & Hell, JW (2009). Supramolecular assemblies and localized regulation of voltage-gated ion channels. *Physiol Rev* **89**: 411-52, 10.1152/physrev.00029.2007.

del Valle-Rodriguez, A, Lopez-Barneo, J & Urena, J (2003). Ca2+ channel-sarcoplasmic reticulum coupling: a mechanism of arterial myocyte contraction without Ca2+ influx. *EMBO J* **22**: 4337-45, 10.1093/emboj/cdg432.

Dhillon, R (2012). The management of neonatal pulmonary hypertension. *Arch Dis Child Fetal Neonatal Ed* **97**: F223-8, 10.1136/adc.2009.180091.

Dumitrescu, D, Seck, C, ten Freyhaus, H, Gerhardt, F, Erdmann, E & Rosenkranz, S (2011). Fully reversible pulmonary arterial hypertension associated with dasatinib treatment for chronic myeloid leukaemia. *Eur Respir J* **38**: 218-20, 10.1183/09031936.00154210.

Duprat, F, Lauritzen, I, Patel, A & Honore, E (2007). The TASK background K2P channels: chemo- and nutrient sensors. *Trends Neurosci* **30**: 573-80, 10.1016/j.tins.2007.08.003.

Enyeart, JJ, Danthi, SJ, Liu, H & Enyeart, JA (2005). Angiotensin II inhibits bTREK-1 K+ channels in adrenocortical cells by separate Ca2+- and ATP hydrolysis-dependent mechanisms. *J Biol Chem* **280**: 30814-28, 10.1074/jbc.M504283200.

Evans, AM, Osipenko, ON & Gurney, AM (1996). Properties of a novel K+ current that is active at resting potential in rabbit pulmonary artery smooth muscle cells. *J Physiol* **496 (Pt 2)**: 407-20.

Ghofrani, HA, Distler, O, Gerhardt, F, Gorenflo, M, Grunig, E, Haefeli, WE*, et al.* (2010a). Treatment of pulmonary arterial hypertension (PAH): recommendations of the Cologne Consensus Conference 2010. *Dtsch Med Wochenschr* **135 Suppl 3**: S87-101, 10.1055/s-0030-1263316.

Ghofrani, HA, Morrell, NW, Hoeper, MM, Olschewski, H, Peacock, AJ, Barst, RJ*, et al.* (2010b). Imatinib in pulmonary arterial hypertension patients with inadequate response to established therapy. *Am J Respir Crit Care Med* **182**: 1171-7, 10.1164/rccm.201001-0123OC.

Giaid, A, Michel, RP, Stewart, DJ, Sheppard, M, Corrin, B & Hamid, Q (1993). Expression of endothelin-1 in lungs of patients with cryptogenic fibrosing alveolitis. *Lancet* **341**: 1550-4.

Gurney, A, Manoury, B (2009). Two-pore potassium channels in the cardiovascular system. *Eur Biophys J* **38**: 305-18, 10.1007/s00249-008-0326-8.

Gurney, AM, Osipenko, ON, MacMillan, D & Kempsill, FE (2002). Potassium channels underlying the resting potential of pulmonary artery smooth muscle cells. *Clin Exp Pharmacol Physiol* **29**: 330-3.

Gurney, AM, Osipenko, ON, MacMillan, D, McFarlane, KM, Tate, RJ & Kempsill, FE (2003). Two-pore domain K channel, TASK-1, in pulmonary artery smooth muscle cells. *Circ Res* **93**: 957-64, 10.1161/01.RES.0000099883.68414.61.

Holmes, TC, Berman, K, Swartz, JE, Dagan, D & Levitan, IB (1997). Expression of voltage-gated potassium channels decreases cellular protein tyrosine phosphorylation. *J Neurosci* **17**: 8964-74.

Holmes, TC, Fadool, DA, Ren, R & Levitan, IB (1996). Association of Src tyrosine kinase with a human potassium channel mediated by SH3 domain. *Science* **274**: 2089-91.

Hulme, JT, Coppock, EA, Felipe, A, Martens, JR & Tamkun, MM (1999). Oxygen sensitivity of cloned voltage-gated K(+) channels expressed in the pulmonary vasculature. *Circ Res* **85**: 489-97.

Jensen, KS, Micco, AJ, Czartolomna, J, Latham, L & Voelkel, NF (1992). Rapid onset of hypoxic vasoconstriction in isolated lungs. *J Appl Physiol* **72**: 2018-23.

Kang, D, Han, J & Kim, D (2006). Mechanism of inhibition of TREK-2 (K2P10.1) by the Gq-coupled M3 muscarinic receptor. *Am J Physiol Cell Physiol* **291**: C649-56, 10.1152/ajpcell.00047.2006.

Kantarjian, H, Shah, NP, Hochhaus, A, Cortes, J, Shah, S, Ayala, M*, et al.* (2010). Dasatinib versus imatinib in newly diagnosed chronic-phase chronic myeloid leukemia. *N Engl J Med* **362**: 2260-70, 10.1056/NEJMoa1002315.

Kato, M, Staub, NC (1966). Response of small pulmonary arteries to unilobar hypoxia and hypercapnia. *Circ Res* **19**: 426-40.

Kim, LC, Song, L & Haura, EB (2009). Src kinases as therapeutic targets for cancer. *Nat Rev Clin Oncol* **6**: 587-95, 10.1038/nrclinonc.2009.129.

Kleppisch, T, Nelson, MT (1995). Adenosine activates ATP-sensitive potassium channels in arterial myocytes via A2 receptors and cAMP-dependent protein kinase. *Proc Natl Acad Sci U S A* **92**: 12441-5.

Knock, GA, Shaifta, Y, Snetkov, VA, Vowles, B, Drndarski, S, Ward, JP*, et al.* (2008a). Interaction between src family kinases and rho-kinase in agonist-induced Ca2+-sensitization of rat pulmonary artery. *Cardiovasc Res* **77**: 570-9, 10.1093/cvr/cvm073.

Knock, GA, Snetkov, VA, Shaifta, Y, Drndarski, S, Ward, JP & Aaronson, PI (2008b). Role of src-family kinases in hypoxic vasoconstriction of rat pulmonary artery. *Cardiovasc Res* **80**: 453-62, 10.1093/cvr/cvn209.

Li, Y, Connolly, M, Nagaraj, C, Tang, B, Balint, Z, Popper, H*, et al.* (2012). Peroxisome proliferator-activated receptor-beta/delta, the acute signaling factor in prostacyclin-induced pulmonary vasodilation. *Am J Respir Cell Mol Biol* **46**: 372-9, 10.1165/rcmb.2010-0428OC.

Lopes, CM, Rohacs, T, Czirjak, G, Balla, T, Enyedi, P & Logothetis, DE (2005). PIP2 hydrolysis underlies agonist-induced inhibition and regulates voltage gating of two-pore domain K+ channels. *J Physiol* **564**: 117-29, 10.1113/jphysiol.2004.081935.

Madden, JA, Dawson, CA & Harder, DR (1985). Hypoxia-induced activation in small isolated pulmonary arteries from the cat. *J Appl Physiol* **59**: 113-8.

Mandegar, M, Fung, YC, Huang, W, Remillard, CV, Rubin, LJ & Yuan, JX (2004). Cellular and molecular mechanisms of pulmonary vascular remodeling: role in the development of pulmonary hypertension. *Microvasc Res* **68**: 75-103, 10.1016/j.mvr.2004.06.001.

Mattei, D, Feola, M, Orzan, F, Mordini, N, Rapezzi, D & Gallamini, A (2009). Reversible dasatinib-induced pulmonary arterial hypertension and right ventricle failure in a previously allografted CML patient. *Bone Marrow Transplant* **43**: 967-8, 10.1038/bmt.2008.415.

Miyauchi, T, Yorikane, R, Sakai, S, Sakurai, T, Okada, M, Nishikibe, M*, et al.* (1993). Contribution of endogenous endothelin-1 to the progression of cardiopulmonary alterations in rats with monocrotaline-induced pulmonary hypertension. *Circ Res* **73**: 887-97.

Nakanishi, K, Tajima, F, Osada, H, Nakamura, A, Yagura, S, Kawai, T*, et al.* (1996). Pulmonary, vascular responses in rats exposed to chronic hypobaric hypoxia at two different altitude levels. *Pathol Res Pract* **192**: 1057-67.

Olschewski, A (2010). Targeting TASK-1 channels as a therapeutic approach. *Adv Exp Med Biol* **661**: 459-73, 10.1007/978-1-60761-500-2_30.

Olschewski, A, Hong, Z, Nelson, DP & Weir, EK (2002). Graded response of K+ current, membrane potential, and [Ca2+]i to hypoxia in pulmonary arterial smooth muscle. *Am J Physiol Lung Cell Mol Physiol* **283**: L1143-50, 10.1152/ajplung.00104.2002.

Olschewski, A, Li, Y, Tang, B, Hanze, J, Eul, B, Bohle, RM*, et al.* (2006). Impact of TASK-1 in human pulmonary artery smooth muscle cells. *Circ Res* **98**: 1072-80, 10.1161/01.RES.0000219677.12988.e9.

Peng, W, Hoidal, JR & Farrukh, IS (1999). Role of a novel KCa opener in regulating K+ channels of hypoxic human pulmonary vascular cells. *Am J Respir Cell Mol Biol* **20**: 737-45.

Perez-Garcia, MT, Lopez-Lopez, JR & Gonzalez, C (1999). Kvbeta1.2 subunit coexpression in HEK293 cells confers O2 sensitivity to kv4.2 but not to Shaker channels. *J Gen Physiol* **113**: 897-907.

Platoshyn, O, Yu, Y, Golovina, VA, McDaniel, SS, Krick, S, Li, L*, et al.* (2001). Chronic hypoxia decreases K(V) channel expression and function in pulmonary artery myocytes. *Am J Physiol Lung Cell Mol Physiol* **280**: L801-12.

Post, JM, Hume, JR, Archer, SL & Weir, EK (1992). Direct role for potassium channel inhibition in hypoxic pulmonary vasoconstriction. *Am J Physiol* **262**: C882-90.

Robertson, TP, Aaronson, PI & Ward, JP (2003). Ca2+ sensitization during sustained hypoxic pulmonary vasoconstriction is endothelium dependent. *Am J Physiol Lung Cell Mol Physiol* **284**: L1121-6, 10.1152/ajplung.00422.2002.

Robertson, TP, Hague, D, Aaronson, PI & Ward, JP (2000). Voltage-independent calcium entry in hypoxic pulmonary vasoconstriction of intrapulmonary arteries of the rat. *J Physiol* **525 Pt 3**: 669-80.

Rubin, LJ, Badesch, DB, Barst, RJ, Galie, N, Black, CM, Keogh, A*, et al.* (2002). Bosentan therapy for pulmonary arterial hypertension. *N Engl J Med* **346**: 896-903, 10.1056/NEJMoa012212.

Schermuly, RT, Dony, E, Ghofrani, HA, Pullamsetti, S, Savai, R, Roth, M*, et al.* (2005). Reversal of experimental pulmonary hypertension by PDGF inhibition. *J Clin Invest* **115**: 2811-21, 10.1172/JCI24838.

Shirai, M, Sada, K & Ninomiya, I (1986). Effects of regional alveolar hypoxia and hypercapnia on small pulmonary vessels in cats. *J Appl Physiol* **61**: 440-8.

Stewart, DJ, Levy, RD, Cernacek, P & Langleben, D (1991). Increased plasma endothelin-1 in pulmonary hypertension: marker or mediator of disease? *Ann Intern Med* **114**: 464-9.

Tang, B, Li, Y, Nagaraj, C, Morty, RE, Gabor, S, Stacher, E*, et al.* (2009). Endothelin-1 inhibits background two-pore domain channel TASK-1 in primary human pulmonary artery smooth muscle cells. *Am J Respir Cell Mol Biol* **41**: 476-83, 10.1165/rcmb.2008-0412OC.

Tolins, M, Weir, EK, Chesler, E, Nelson, DP & From, AH (1986). Pulmonary vascular tone is increased by a voltage-dependent calcium channel potentiator. *J Appl Physiol* **60**: 942-8.

Tuder, RM, Chacon, M, Alger, L, Wang, J, Taraseviciene-Stewart, L, Kasahara, Y*, et al.* (2001). Expression of angiogenesis-related molecules in plexiform lesions in severe pulmonary hypertension: evidence for a process of disordered angiogenesis. *J Pathol* **195**: 367-74, 10.1002/path.953.

Vadula, MS, Kleinman, JG & Madden, JA (1993). Effect of hypoxia and norepinephrine on cytoplasmic free Ca2+ in pulmonary and cerebral arterial myocytes. *Am J Physiol* **265**: L591-7.

Wang, J, Juhaszova, M, Rubin, LJ & Yuan, XJ (1997). Hypoxia inhibits gene expression of voltage-gated K+ channel alpha subunits in pulmonary artery smooth muscle cells. *J Clin Invest* **100**: 2347-53, 10.1172/JCI119774.

Weir, EK, Archer, SL (1995). The mechanism of acute hypoxic pulmonary vasoconstriction: the tale of two channels. *FASEB J* **9**: 183-9.

Weir, EK, Cabrera, JA, Mahapatra, S, Peterson, DA & Hong, Z (2010). The role of ion channels in hypoxic pulmonary vasoconstriction. *Adv Exp Med Biol* **661**: 3-14, 10.1007/978-1-60761-500-2_1.

Weir, EK, Olschewski, A (2006). Role of ion channels in acute and chronic responses of the pulmonary vasculature to hypoxia. *Cardiovasc Res* **71**: 630-41, 10.1016/j.cardiores.2006.04.014.

Weissmann, N, Grimminger, F, Walmrath, D & Seeger, W (1995). Hypoxic vasoconstriction in buffer-perfused rabbit lungs. *Respir Physiol* **100**: 159-69.

Yuan, JX, Aldinger, AM, Juhaszova, M, Wang, J, Conte, JV,Jr, Gaine, SP*, et al.* (1998). Dysfunctional voltage-gated K+ channels in pulmonary artery smooth muscle cells of patients with primary pulmonary hypertension. *Circulation* **98**: 1400-6.

Yuan, XJ (1995). Voltage-gated K+ currents regulate resting membrane potential and [Ca2+]i in pulmonary arterial myocytes. *Circ Res* **77**: 370-8.

Yuan, XJ, Goldman, WF, Tod, ML, Rubin, LJ & Blaustein, MP (1993). Hypoxia reduces potassium currents in cultured rat pulmonary but not mesenteric arterial myocytes. *Am J Physiol* **264**: L116-23.

Yuan, XJ, Tod, ML, Rubin, LJ & Blaustein, MP (1995). Hypoxic and metabolic regulation of voltage-gated K+ channels in rat pulmonary artery smooth muscle cells. *Exp Physiol* **80**: 803-13.

Appendix

Publication list:

Nagaraj C, Tang B, Bálint Z, Wygrecka M, Hrzenjak A, Kwapiszewska G, Stacher E, Lindenmann J, Weir EK, Olschewski H, Olschewski A. Src tyrosine kinase is crucial for potassium channel function in human pulmonary arteries. Eur Respir J. 2012 Apr 20.

Zabini D, **Nagaraj C**, Stacher E, Lang IM, Nierlich P, Klepetko W, Heinemann A, Olschewski H, Bálint Z, Olschewski A. Angiostatic factors in the pulmonary endarterectomy material from chronic thromboembolic pulmonary hypertension patients cause endothelial dysfunction. PLoS One. 2012;7(8):e43793.

Li Y, Connolly M, **Nagaraj C**, Tang B, Bálint Z, Popper H, Smolle-Juettner FM, Lindenmann J, Kwapiszewska G, Aaronson PI, Wohlkoenig C, Leithner K, Olschewski H, Olschewski A. Peroxisome proliferator-activated receptor-β/δ, the acute signaling factor in prostacyclin-induced pulmonary vasodilation. Am J Respir Cell Mol Biol. 2012 Mar;46(3):372-9. Epub 2011 Oct 20.

Tang B, Li Y, **Nagaraj C**, Morty RE, Gabor S, Stacher E, Voswinckel R, Weissmann N, Leithner K, Olschewski H, Olschewski A. Endothelin-1 inhibits background two-pore domain channel TASK-1 in primary human pulmonary artery smooth muscle cells. Am J Respir Cell Mol Biol. 2009 Oct;41(4):476-83.